Heavy quarkonia in quark-gluon plasma

Cheuk-Yin Wong
Physics Division, Oak Ridge National Laboratory, Oak Ridge, Tennessee 37831, USA
and Department of Physics, University of Tennessee, Knoxville, Tennessee 37996, USA
(Received 2 August 2004; revised manuscript received 3 May 2005; published 29 September 2005)

Using the color-singlet free energy F_1 and total internal energy U_1 obtained by Kaczmarek *et al.* (hep-lat/0309121) for a static quark Q and an antiquark $\bar{Q}$ in quenched QCD, we study the binding energies and wave functions of heavy quarkonia in a quark-gluon plasma. By minimizing the grand potential in a simplified schematic model, we find that the proper color-singlet Q-$\bar{Q}$ potential can be obtained from the total internal energy U_1 by subtracting the gluon internal energy contributions. We carry out this subtraction in the local energy-density approximation in which the gluon energy density can be related to the local gluon pressure by the quark-gluon plasma equation of state. We find in this approximation that the proper color-singlet Q-$\bar{Q}$ potential is approximately F_1 for $T \sim T_c$ and it changes to $\frac{3}{4}F_1 + \frac{1}{4}U_1$ at high temperatures. In this potential model, the J/ψ is weakly bound above the phase-transition temperature T_c, and it dissociates spontaneously above $1.62T_c$, whereas χ_c and ψ' are unbound in the quark-gluon plasma. The bottomium states Υ, χ_b, and Υ' are bound in the quark-gluon plasma and they dissociate at $4.1T_c$, $1.18T_c$, and $1.38T_c$ respectively. For comparison, we evaluate the heavy quarkonium binding energies also in other models using the free energy F_1 or the total internal energy U_1 as the Q-$\bar{Q}$ potential. The comparison shows that the model with the new Q-$\bar{Q}$ potential proposed here gives dissociation temperatures that agree best with those from spectral function analyses. We evaluate the cross section for $\sigma(g + J/\psi \to c + \bar{c})$ and its inverse process to determine the J/ψ dissociation width and the rate of J/ψ production by recombining c and $\bar{c}$ in the quark-gluon plasma.

DOI: 10.1103/PhysRevC.72.034906 PACS number(s): 25.75.Dw

I. INTRODUCTION

The stability of heavy quarkonia in the quark-gluon plasma is an interesting subject of current research in high-energy heavy-ion collisions as Matsui and Satz have suggested that the suppression of J/ψ production can be used as a signature of the quark-gluon plasma [1]. DeTar [2,3], Hansson, Lee, and Zahed [4], and Simonov [5–7] argued however that because the range of the strong interaction is not likely to change drastically across the phase transition, low-lying mesons including J/ψ may remain in relatively narrow states and the suppression of J/ψ is not a signature of the deconfinement phase transition [3]. Whether or not J/ψ production will be suppressed depends on the screening between the heavy quark Q and the heavy antiquark $\bar{Q}$ when the quarkonium is placed in the quark-gluon plasma. The degree of screening is highly nonperturbative at temperatures near the phase-transition temperature [8]. The related question of quarkonium stability must be examined in nonperturbative QCD using, for example, lattice gauge theory.

Recent investigations of masses and widths of heavy quarkonia in quenched lattice QCD calculations were carried out by Asakawa and Coworkers [9,10] and Petreczky *et al.* [11–13] using the spectral function analysis and the maximum entropy method. They found that the width of J/ψ remains relatively narrow up to 1.6 times the critical phase-transition temperature T_c. Reconsidering the properties of the quark-gluon plasma also led Zahed and Shuryak to suggest that quark-gluon plasma at temperatures up to a few T_c supports weakly bound meson states [14–17]. They have also estimated the binding energy of J/ψ and found it to be stable up to $2.7T_c$ [15]. The possibility of weakly bound meson states in the quark-gluon plasma was suggested earlier by DeTar [2,3] and Hatsuda and Kunihiro [18]. Phenomenological discussions on medium modifications of charmonium in high-energy heavy-ion collisions have been presented recently by Grandchamp, Rapp, and Brown [19]. Summaries of recent developments in heavy quarkonium suppression and deconfinement have also been reported by Petreczky [20] and Karsch [21].

Because knowledge of the stability of J/ψ has important implications on the fate of J/ψ in the quark-gluon plasma, it is important to obtain an independent assessment of the binding of heavy quarkonia, in addition to those from previous analyses. Spectral function analyses of heavy quarkonia using gauge-invariant current-current correlators have been carried out in the quenched approximation. Within the quenched approximation, independent lattice gauge calculations have also been carried out using the correlation of Polyakov lines, from which the free energy F_1 and the total internal energy U_1 can be calculated [22]. The two-body potential obtained from lattice gauge theory can be used to study the dissociation of heavy quarkonia. It is of interest to ask whether, within the same quenched approximation, the spectral function analysis and the potential model analysis will lead to consistent results concerning the stability of quarkonia in the quark-gluon plasma. As we shall deal with lattice results from quenched QCD only, the quark-gluon plasma we shall consider consists of gluons. For convenience, we shall continue to refer to such a gluon medium from quenched QCD as a quark-gluon plasma.

Besides checking the consistency of independent quenched lattice gauge calculations, we would like to use the potential model to examine many physical quantities of interest. If quarkonia is indeed stable in the plasma, it is useful to find

 ©2005 The American Physical Society

out how strongly bound they are. Furthermore, J/ψ can dissociate by collision with constituents of the plasma. In such a collisional dissociation, the rate of dissociation depends on the cross section for the reaction $g + J/\psi \to c + \bar{c}$. We would like to evaluate this cross section as a function of temperature T, which can be obtained by using the bound-state wave functions in the potential model. Knowledge of the dissociation cross section allows a determination of the collisional dissociation width.

In energetic heavy-ion collisions, many pairs of charm quarks and antiquarks may be produced in a single central collision [23,24]. These charm quarks and antiquarks can recombine to form J/ψ in the quark-gluon plasma. We also wish to find out the rate of producing J/ψ through such a reaction. The production rate depends on the cross section for the reaction $c + \bar{c} \to J/\psi + g$. The latter quantity can be obtained from the cross section for the inverse reaction $g + J/\psi \to c + \bar{c}$, which we already intend to calculate.

Previously, the effects of temperature on the stability of heavy quarkonium was studied by Digal *et al.* [25,26] and Wong [27,28] using the free energy and assuming that the effects of entropy are small. It was, however, pointed out by Zantow, Kaczmarek, Karsch, and Petreczky [8,29,30] that the effects of entropy depend on the separation distance between c and $\bar{c}$. They suggested that the total internal energy U_1, instead of the free energy F_1, may be used as the $Q\bar{Q}$ potential for the calculation of heavy quarkonium bound states. As the theoretical basis for this suggestion has not been fully explained in the literature, we shall go into details to examine the theoretical questions on the proper potential for Q-$\bar{Q}$ states. We find that the proper Q-$\bar{Q}$ potential involves the Q and $\bar{Q}$ internal energy $U^{(1)}_{Q\bar{Q}}$. We shall show that in the local energy-density approximation, $U^{(1)}_{Q\bar{Q}} = 3F_1/(3+a) + aU_1/(3+a)$, where $a = 3p/\epsilon$ is given by the quark-gluon plasma equation of state.

When a heavy quarkonium is placed in a quark-gluon plasma, in the conventional description it is assumed that the medium effect is dominated by the effect of Debye screening [1,8], which leads to a decrease in the attractive interaction between the heavy quark and antiquark. We would like to study the effects of antiscreening resulting from the deconfined gluons and the relationship between antiscreening and the area law of spatial Polyakov loops [2,3,31,33,34]. We would like to show that because the Gauss law of QCD contains a nonlinear term involving the gluon field, the gluon field induces color charges at the field points. These induced color charges act to antiscreen the interaction between the heavy quark and the antiquark. We shall show that the strength of the antiscreening effect increases with an increase in the gluon correlation length and is proportional quadratically to the magnitude of the gluon fields. The antiscreening effects resulting from deconfined gluons bring an additional degree of freedom to mediate the interaction between the quark and the antiquark.

This paper is organized as follows. In Sec. II, we review the heavy quarkonium production mechanism and the thermalization of the quark-gluon medium in high-energy heavy-ion collisions. We examine the evidence for rapid thermalization as revealed by the elliptic flow and hydrodynamics. In Sec. III, we review the lattice gauge calculations for the interaction between a heavy quark and a heavy antiquark and the gauge dependence of the interaction in bound-state problems. In Sec. IV, we show that the total internal energy U_1 contains contributions from the internal energy of the Q-$\bar{Q}$ pair and the internal energy of the gluons. In Sec. V, we use an appropriate variational principle to obtain the equation of motion for the quarkonium single-particle states and find that the proper Q-$\bar{Q}$ potential involves only the Q-$\bar{Q}$ internal energy. To obtain the internal energy of the heavy quark pair, the gluon internal energy must be subtracted from the total internal energy U_1. In Sec. VI we show how such a subtraction can be carried out in the local energy-density approximation, using the quark-gluon plasma equation of state and the first law of thermodynamics. In Sec. VII, we show how the color-singlet F_1 and U_1 obtained by Kaczmarek *et al.* [22] in quenched QCD can be parametrized and the proper Q-$\bar{Q}$ potential can be obtained as a linear combination of F_1 and U_1 from the lattice gauge results. Using this heavy quark-antiquark potential, we calculate the eigenenergies and eigenfunctions for charmonia in the quark-gluon plasma as a function of temperature in Sec. VIII. The locations of the dissociation temperatures at which heavy quarkonia begin to be unbound are then determined. The heavy quarkonium dissociation temperatures are compared with those determined from spectral function analyses. In Sec. IX, we calculate the eigenenergies and eigenfunctions for $b\bar{b}$ bound states in the quark-gluon plasma as a function of temperature. We discuss the effects of antiscreening resulting from deconfined gluons in the quark-gluon plasma in Sec. X. In Sec. XI, we discuss how the J/ψ bound-state wave function can be used to calculate the cross section for $g + J/\psi \to c + \bar{c}$ after the J/ψ absorbs an $E1$ gluon, using the formulation of gluon dissociation cross section presented previously [28]. The dissociation cross sections and collisional dissociation widths of J/ψ in the quark-gluon plasma are then determined as a function of temperature in Sec. XII. In Sec. XIII, we evaluate the cross section for the inverse process of $c + \bar{c} \to J/\psi + g$ using the cross section of $g + J/\psi \to c + \bar{c}$ obtained in Sec. XII. The rate of J/ψ production by recombining c and $\bar{c}$ in a quark-gluon plasma is estimated. We conclude our discussion in Sec. XIV. In the Appendix, we show that the integral of the gauge fields along a spacelike Polyakov loop obeys an area law if the gauge fields are correlated. This result is used in Sec. X to explain the antiscreening effect.

II. HEAVY QUARKONIA PRODUCTION AND THE THERMALIZATION OF THE MEDIUM

We are interested in using a heavy quarkonium to probe the properties of the matter produced in central high-energy heavy-ion collisions. In the collider frame, the colliding nuclei have the shape of Lorentz-contracted disks. The collisions are known to be highly inelastic in which a large fraction of the incident collision energy is released after the collision. What is the rate of the relaxation of the initial configuration to thermal equilibrium?

From the experimental viewpoint, recent RHIC experiments by the STAR [35], PHENIX [36], and PHOBOS [37]

Collaborations reveal the presence of an elliptic collective flow in noncentral Au-Au collisions at RHIC energies. The occurrence of such a flow indicates that the initial azimuthally symmetric momentum distribution of particles is deformed into an azimuthally asymmetric momentum distribution. The magnitude of the azimuthally asymmetry is sensitive to the time at which the free streaming of particles terminates and the dynamics of a thermally equilibrated system begins [38–40]. Too late a thermalization time will lead to a spatially more extended system with a lower pressure gradient and a smaller azimuthal asymmetry. The azimuthal asymmetry is also sensitive to the number of degrees of freedom in the equation of state. The magnitude of the asymmetry can be well explained in terms of a hydrodynamical model of the quark-gluon plasma by assuming thermalization at an initial time about 0.6 fm/c [38]. We infer from the experimental elliptic flow data and its hydrodynamical description that the thermalization in the central region of a RHIC nucleus-nucleus collision is very rapid, as short as 0.6 fm/c after the collision.

From theoretical viewpoints, it was first pointed out by Landau [41] that the initial configuration after a high-energy nuclear collision consists of matter at an extremely high energy density in a very thin disk. The great magnitude of the energy density means that the number density of quanta of matter is very large. Such a large number density in a thin disk of matter leads to a very small mean free path compared to its dimensions, leading to a rapid relaxation to thermal equilibrium. According to Landau, "in the course of time, the system expands, the property of the small mean-free path must be valid also for a significant part of the process of expansion and this part of the expansion process must have hydrodynamical character" [41]. Landau hydrodynamics provides a reasonable description of the widths of the rapidity distribution for high-energy hadron-hadron and nucleus-nucleus collisions from $\sqrt{s} = 3$ GeV to RHIC collisions at 200 GeV [42,43]. A hydrodynamical description with a rapid thermal relaxation also provides a good description of the elliptic flow of matter after a Au-Au collision at RHIC, as previously indicated.

It is also useful to point out that not only does quanta in nonequilibrium QCD matter interact with other quanta (gluons and quarks) in two-body processes in terms of two-body collisions, but the quanta also interact with the fields generated by all other quanta. Because of the non-Abelian nature of the QCD interaction, the fields generated by other quanta are also sources of color fields and the quanta must in addition interact with the color fields generated by the fields of all other particles, in a highly nonlinear manner (see Sec. X for another manifestation of the nonlinear nature of the gauge field). Thus, quanta interact with other quanta not only by direct short-range two-body collisions but also by highly nonlocal action-at-a-distance long-range interactions, through the fields generated by the fields of other quanta. There is thus an additional nonlinear and long-range mechanism of thermalization in non-Abelian interactions that provides an extra push for rapid relaxation to thermal equilibrium.

The rate of thermalization of a quark-gluon system after an ultrarelativistic heavy-ion collision is the subject of current theoretical research and has been discussed by Wong [44] and Molnar and Gyulassy [45]. The small mean free path has also been discussed by Shuryak [46] and Gyulassy and McLerran [47] (see also Ref. [48]). The focus of the research is on trying to understand the phenomenologically fast rate of thermalization as indicated be the experimental elliptic flow evidence. For example, Molnar and Gyulassy [45], found it necessary to shorten the parton mean free path by an order of magnitude to reproduce the magnitude of the elliptic flow. Similarly, in parton cascade, Lin, Ko, and Pal [49] found it necessary to increase the parton-parton cross section by a large factor to describe the dynamics in nucleus-nucleus collisions at RHIC.

To use heavy quarkonia as a probe of the quark-gluon plasma, we need knowledge of the heavy-quarkonium production mechanism. In a nucleus-nucleus collision at high energies, the partons of one nucleon and the partons of another nucleon can collide to produce occasionally a heavy quark-antiquark pair. The time scale for the production is of the order of $\hbar/2m_Q$, where m_Q is the mass of the heavy quark. It is of order 0.06 fm/c for a c-$\bar{c}$ pair and of order 0.02 fm/c for a b-$\bar{b}$ pair. As the initial partons carry varying fractions of the initial momenta of the colliding nucleons, the heavy quark pair will come out at different energies. Depending on the Feynman diagram of the production process, the produced Q-$\bar{Q}$ pair after the hard scattering process may be in a purely color-singlet quarkonia state or a coherent admixture of color-singlet and color-octet states [50,51]. The projection of different final states from a coherent admixture gives the probability amplitude for the occurrence of the final states. A color-octet state will need to emit a soft gluon of energy E_{gluon} to become subsequently a color-singlet state in an emission time of order $\hbar/E_{\text{gluon}}$. For the emission of soft gluon of a few hundred MeV, the time for the emission is of order 0.5–1.0 fm/c.

From these considerations on the rapid thermalization of the quark-gluon plasma and the time for the production of heavy quarkonia, one envisages that, by the time the colliding matter is thermalized at about 0.6 fm/c, a large fraction of the quarkonia has already been formed, although in various energy states. The quark-gluon plasma is expected to have a lifetime of a few fm/c, which is longer than the heavy quarkonium orbital period of order $\hbar/(0.5\text{ GeV})$. It is therefore meaningful to study the fate of a produced heavy quarkonia in a thermalized quark-gluon plasma at a finite temperature. The behavior of the heavy quarkonium system before the quark-gluon plasma reaches thermal equilibrium and the interaction of a coherent Q-$\bar{Q}$ color admixture in the thermalized quark-gluon plasma are topics that are beyond the scope of the investigation of the present manuscript.

It should be pointed out that for a heavy quarkonium system in a quark-gluon plasma the thermalization of the quark-gluon medium does not necessarily imply the thermalization of the heavy quarkonium system. The former arises from the interaction among the light quarks and gluons, whereas the latter depends on the interaction between the heavy quarkonium and the constituents of the quark-gluon plasma. Our previously mentioned evidence concerning the rapid thermalization refers to the thermalization of the quark-gluon plasma and not necessarily to the thermalization of the heavy quarkonium system in the quark-gluon plasma. If an isolated heavy quarkonium is placed in the thermalized

quark-gluon plasma, the heavy quarkonium system is not in thermal equilibrium with the medium. It will interact with the medium as its density matrix will evolve with time. Given a sufficient time that is longer than the heavy quarkonium thermalization time, the heavy quarkonium will also reach thermal equilibrium with its thermalized quark-gluon plasma. The thermalization status of a heavy quarkonium system can be inferred from the occupation number distribution of heavy quarkonium single-particle states. The occupation numbers in a thermalized heavy-quarkonium system will obey a Bose-Einstein distribution characterized by temperature. In our present work, we shall study both a thermalized heavy quarkonium system and an isolated $Q\bar{Q}$ bound state in the quark-gluon plasma.

III. LATTICE GAUGE CALCULATIONS

In a quark-gluon plasma, a quarkonium is actually a heavy quark and a heavy antiquark each surrounded by a cloud of gluons and quarks. In the quenched approximation in which there are no dynamical quarks, the cloud surrounding the heavy quark and antiquark is approximated to consist of gluons only. Because gluons are involved, the quark-antiquark system will be in different color states at different instances. We shall be interested in those systems in which the heavy quark and antiquark exist in the color-singlet state. Only in the color-singlet state will be the effective interaction between a quark (plus its cloud) and an antiquark (plus its cloud) be attractive. Such a color-singlet system can further absorb a gluon and become a color-octet system and we shall also study the cross section for such a process.

The interaction between a heavy quark and a heavy antiquark in the color-singlet state was studied by Kaczmarek, Karsch, Petreczky, and Zantow [22]. They calculated $\langle \mathrm{tr} L(\mathbf{r}/2) L^\dagger(-\mathbf{r}/2)\rangle$ in the quenched approximation and they obtained the color-singlet free energy $F_1(\mathbf{r}, T)$ from

$$\langle \mathrm{tr} L(\mathbf{r}/2) L^\dagger(-\mathbf{r}/2)\rangle = e^{-F_1(\mathbf{r},T)/kT}, \tag{1}$$

where $\mathrm{tr} L(\mathbf{r}/2)L^\dagger(-\mathbf{r}/2)$ is the trace of the product of two Polyakov lines at $\mathbf{r}/2$ and $-\mathbf{r}/2$. The quark and the antiquark lines do not, in general, form a close loop. As a gauge transformation introduces phase factors at the beginning and the end of an open Polyakov line, $\langle \mathrm{tr} L(\mathbf{r}/2)L^\dagger(-\mathbf{r}/2)\rangle$ is not gauge invariant under a gauge transformation. Calculations have been carried out in the Coulomb gauge, which is the proper gauge to study bound states.

It should be noted that although the interaction between the quark and the antiquark is gauge dependent, the bound state energies are physical quantities and they do not depend on the gauge. As we explain in the following, a judicial choice of the Coulomb gauge in the bound-state calculation will help in avoiding spurious next-to-leading contributions and singularities, which can be removed in other gauges only by additional laborious effort [52–54].

To study the bound states of a heavy quarkonium, we need a bound-state equation, such as the Bethe-Salpeter equation, and the interaction kernel in the equation. The nonrelativistic approximation of the Bethe-Salpeter equation leads to the usual Schrödinger equation with the gauge-boson-exchange interaction [55,56]. It is necessary to choose a gauge to specify the gauge-boson-exchange interaction. We can consider the case of QED, from which we can get good insight into the gauge dependence. For the static nonrelativistic problem, the natural choice in the gauge-boson-exchange potential is the Coulomb gauge, in which the $1/\mathbf{q}^2$ behavior is found in single-Coulomb photon exchange. The binding energy, which is of order α^2, has corrections only in the α^4 order. It gives the correct Breit equation with the proper spin properties when we expand the interaction to the next order. Graphs with the cross two-Coulomb-exchange diagrams vanish in the static limit, and uncrossed multiple Coulomb exchanges are strictly iterations of the potential [52]. In any other gauge, the zero-zero component of the photon propagator has some residual noninstantaneous contributions. A large number of Bethe-Salpeter kernels need to be included to eliminate the spurious contributions in the next order of α^3 and $\alpha^3/\ln\alpha$ corrections [53,54]. Therefore, in their work on the static potential in QCD, Appelquist, Dine, and Muzinich [52] suggested that the gauge freedom can be used to eliminate spurious long-range forces at the outset. They found that the Coulomb gauge continues to be useful in the static potential in QCD. The dynamics is now considerably complicated but spurious contributions are still eliminated [52].

Thus, it is therefore important to recognize, as in QED, that there is a gauge dependence in the two-body bound-state potential in the Bethe-Salpeter equation but it is most appropriate to solve the bound-state problem using two-body potentials obtained in the Coulomb gauge, as was obtained by Kaczmarek *et al*. [22].

IV. HEAVY QUARKONIUM STATES IN A THERMALIZED QUARK-GLUON PLASMA

The state of a heavy quarkonium in a quark-gluon plasma can be described by a density matrix. The set of single-particle states for this density matrix can be chosen such that they can be represented well by quarkonium states in a Q-$\bar{Q}$ potential, and the residual interaction between the gluons with the quarkonium can be treated as a perturbation. In this single-particle basis, the heavy quarkonium density matrix can be approximated to contain only diagonal matrix elements representing the probabilities for the occupation of different single-particle states. What is the Q-$\bar{Q}$ potential that enters into the Schrödinger equation for these quarkonium single-particle states?

The Q-$\bar{Q}$ potential in perturbative QCD has been studied by Petreczky [20]. We would like to examine here the Q-$\bar{Q}$ potential in nonperturbative lattice QCD calculations. In previous analyses, the Q-$\bar{Q}$ potential was taken to be the free energy F_1 for a pair of correlated Polyakov lines, assuming that the effects of entropy are small [25–28]. It was, however, pointed out by Zantow, Kaczmarek, Karsch, and Petreczky [8,29,30] that the effects of entropy are large and the total internal energy U_1, may be used as the Q-$\bar{Q}$ potential. As the theoretical basis for these suggestions has not been fully discussed in the literature, we shall go into details of the proper description of the Q-$\bar{Q}$ potential and single-particle states.

We start first by studying the auxiliary problem of a *static* color-singlet Q-$\bar{Q}$ pair at a separation $\mathbf{r}$ in a thermalized quark-gluon plasma. In the quenched approximation, the color-singlet free energy $F_1(\mathbf{r}, T)$ for such a static pair can be written from Eq. (1) explicitly in the Euclidean time $\tau = it$ as [31]

$$e^{-\beta F_1(\mathbf{r},T)} = Z(\mathbf{r}, T)/Z_0(T), \tag{2}$$

$$Z(\mathbf{r}, T) = \int [dA] W_{Q\bar{Q}}(A, T, \mathbf{r}), \tag{3}$$

$$Z_0(T) = \int [dA] W_0(A, T), \tag{4}$$

$$W_{Q\bar{Q}}(A, T, \mathbf{r}) = \mathrm{tr}\left\{\hat{P} \exp\left[\int_0^\beta g(\tau) d\tau A_0(\mathbf{r}/2, \tau)\right] \times \exp\left[\int_\beta^0 g(\tau) d\tau A_0(-\mathbf{r}2, \tau)\right]\right\} W_0(A, T), \tag{5}$$

$$W_0(A, T) = \exp\left\{-\frac{1}{4}\int_0^\beta d\tau \int d^3x F_{\mu\nu}F^{\mu\nu}\right\}, \tag{6}$$

where $\beta = 1/kT$ is the inverse temperature, $Z(\mathbf{r}, T)$ is the partition function when a color-singlet Q and $\bar{Q}$ separated by a distance $\mathbf{r}$ is placed in the gluon medium, and $Z_0(T)$ is the partition function in the absence of Q and $\bar{Q}$. The operator $\hat{P}$ is the path-order operator, which is the time-order operator $\hat{T}$ for $\exp\{\int_0^\beta g(\tau) d\tau A_0(\mathbf{r}/2, \tau)\}$ and is the reverse time-order operator for $\exp\{\int_\beta^0 g(\tau) d\tau A_0(-\mathbf{r}/2, \tau)\}$. The free energy $F_1(\mathbf{r}, T)$ with the Q-$\bar{Q}$ pair is measured relative to the free energy $F_0(T)$ without the Q-$\bar{Q}$ pair. We rewrite Eq. (2) as

$$Z_0(T) = \int [dA] e^{\beta F_1(\mathbf{r},T)} \mathrm{tr}\left\{\hat{P} \exp\left[\int_0^\beta g(\tau) d\tau A_0(\mathbf{r}/2, \tau)\right] \times \exp\left[\int_\beta^0 g(\tau) d\tau A_0(-\mathbf{r}/2, \tau)\right]\right\} \times \exp\left\{-\frac{1}{4}\int_0^\beta d\tau \int d^3x F_{\mu\nu}F^{\mu\nu}\right\}. \tag{7}$$

Taking the derivative of this equation with respect to β, we obtain for the derivative of the left-hand side,

$$\frac{\partial\{\mathrm{LHS}\}}{\partial\beta} = \frac{\partial Z_0(T)}{\partial\beta} = \int [dA] \left\{-\frac{1}{4}\int d^3x F_{\mu\nu}F^{\mu\nu}\right\} W_0(A, T), \tag{8}$$

and for the derivative of the right-hand side, we get

$$\frac{\partial\{\mathrm{RHS}\}}{\partial\beta} = \int [dA] e^{\beta F_1(\mathbf{r},T)} \left[\left\{F_1(\mathbf{r}, T) + \beta\frac{\partial F_1(\mathbf{r}, T)}{\partial\beta} - \frac{1}{4}\int d^3x F_{\mu\nu}F^{\mu\nu}\right\} W_{Q\bar{Q}}(A, T, \mathbf{r}) + \mathrm{tr}\left\{g(T)(A_0(\mathbf{r}/2, T) - A_0(-\mathbf{r}/2, T))\hat{P} \times \exp\left[\int_0^\beta g(\tau) d\tau A_0(\mathbf{r}/2, \tau)\right] \times \exp\left[\int_\beta^0 g(\tau) d\tau A_0(-\mathbf{r}/2, \tau)\right]\right\} W_0(A, T)\right]. \tag{9}$$

We equate Eq. (8) to Eq. (9). Using $e^{\beta F_1(\mathbf{r},T)} = Z_0(T)/Z(\mathbf{r}, T)$ and dividing the resultant equation by $Z_0(T)$, we obtain the proper thermodynamic equality relating F_1, S_1, and U_1, for a system with a color-singlet Q and $\bar{Q}$ separated $\mathbf{r}$ at temperature T,

$$F_1(\mathbf{r}, T) + TS_1(\mathbf{r}, T) = U_1(\mathbf{r}, T), \tag{10}$$

where $S_1(\mathbf{r}, T) = -\partial F_1(\mathbf{r}, T)/\partial T$ is the color-singlet entropy with the Q-$\bar{Q}$ pair and is measured relative to the entropy $S_0(T) = -\partial F_0(T)/\partial T$ without the Q-$\bar{Q}$ pair, and $U_1(\mathbf{r}, T)$ is the total color-singlet internal energy given explicitly by

$$U_1(\mathbf{r}, T) = U^{(1)}_{Q\bar{Q}}(\mathbf{r}, T) + U^{(1)}_g(\mathbf{r}, T) - U_{g0}(T), \tag{11}$$

$$U_{g0}(T) = \int [dA] \left\{\frac{1}{4}\int d^3x F_{\mu\nu}F^{\mu\nu}\right\} W_0(A, T) \div \int [dA] W_0(A, T), \tag{12}$$

$$U^{(1)}_g(\mathbf{r}, T) = \int [dA] \left\{\frac{1}{4}\int d^3x F_{\mu\nu}F^{\mu\nu}\right\} W_{Q\bar{Q}}(A, T, \mathbf{r}) \div \int [dA] W_{Q\bar{Q}}(A, T, \mathbf{r}), \tag{13}$$

and

$$U^{(1)}_{Q\bar{Q}}(\mathbf{r}, T) = \int [dA] \mathrm{tr}\left\{g(T)[A_0(\mathbf{r}/2, T) - A_0(-\mathbf{r}/2, T)]\hat{P} \times \exp\left[\int_0^\beta g(\tau) d\tau A_0(\mathbf{r}/2, \tau)\right] \times \exp\left[\int_\beta^0 g(\tau) d\tau A_0(-\mathbf{r}/2, \tau)\right]\right\} W_0(A, T) \div \int [dA] \mathrm{tr}\left\{\hat{P} \exp\left[\int_0^\beta g(\tau) d\tau A_0(\mathbf{r}/2, \tau)\right] \times \exp\left[\int_\beta^0 g(\tau) d\tau A_0(-\mathbf{r}/2, \tau)\right]\right\} W_0(A, T). \tag{14}$$

We may attempt to give names to the various mathematical expressions. In Euclidean time, the quantity $F_{\mu\nu}F^{\mu\nu}/4$ is equal to $(\mathbf{E}^2 + \mathbf{B}^2)/2$, the gluon energy density [31,32]. The quantity $U_{g0}(T)$ is the expectation value of $\int d^3x(\mathbf{E}^2 + \mathbf{B}^2)/2$ with the weight function $W_0(A, T)$, and it corresponds to the gluon internal energy in the absence of the heavy quark pair. It is independent of the separation $\mathbf{r}$ between Q and $\bar{Q}$. In contrast, $U^{(1)}_g(\mathbf{r}, T)$ is the expectation value of $\int d^3x(\mathbf{E}^2 + \mathbf{B}^2)/2$ with the weight function $W_{Q\bar{Q}}(A, T, \mathbf{r})$, and it corresponds to the gluon internal energy in the presence of the heavy quark pair. Consequently, $U^{(1)}_g(\mathbf{r}, T)$ depends on the separation $\mathbf{r}$ between Q and $\bar{Q}$. The difference between the total internal energy U_1 and gluon internal energy difference $U^{(1)}_g(\mathbf{r}, T) - U_{g0}(T)$ is the quantity $U^{(1)}_{Q\bar{Q}}(\mathbf{r}, T)$, the internal energy of the heavy quark pair, including the interaction between Q and $\bar{Q}$ as well as the interaction between Q with gluons and $\bar{Q}$ with gluons.

Equations (10)–(14) show that the total internal energy $U^{(1)}(\mathbf{r}, T)$ contains the gluon internal energy difference $U^{(1)}_g(\mathbf{r}, T) - U_{g0}(T)$. To obtain the $\mathbf{r}$ dependence of the

internal energy of the heavy quark pair $U^{(1)}_{Q\bar{Q}}(\mathbf{r}, T)$, it is necessary to subtract the gluon internal energy difference $U^{(1)}_g(\mathbf{r}, T) - U_{g0}(T)$ from the total internal energy $U_1(\mathbf{r}, T)$. In Sec. VI we shall show a method to carry out such a subtraction in the local energy-density approximation.

V. EQUATION OF MOTION FOR Q-$\bar{Q}$ SINGLE-PARTICLE STATES

Lattice gauge calculations provide information on the free energy F_1 and the total internal energy U_1 for a static color-singlet Q and $\bar{Q}$ separated by a distance $\mathbf{r}$. Quantities for Q and $\bar{Q}$ in the color-octet state can be similarly obtained. For simplicity, we shall limit our consideration to a system of color-singlet Q-$\bar{Q}$ states. The generalization to a system color-octet states can be easily carried out.

We use an appropriate variational principle to obtain the equation of motion for the color-singlet quarkonium states in a quark-gluon plasma. For such a purpose, we consider a schematic toy model that retains the relevant features of the system. In the quenched approximation without dynamical light quarks, the quark-gluon plasma consists of gluons only. The quark Q and antiquark $\bar{Q}$ are in dynamical motion in different single-particle states. For simplicity, we presume that the color degree of freedom has been integrated out. The dynamical degrees of freedom in our schematic model are then the Q-$\bar{Q}$ and gluon states, $\psi_i(\mathbf{r})$ and $\phi_i(\mathbf{r})$, which can be bound or unbound, the corresponding Q-$\bar{Q}$ and gluon state occupation numbers, $n_i(Q\bar{Q})$ and $n_j(g)$, and the total number of gluons, N_g. In the schematic toy model, we represent the Q-$\bar{Q}$, Q-g, $\bar{Q}$-g, and g-g interactions when Q and $\bar{Q}$ belong to a color-singlet state by $V_{Q\bar{Q}}$, V_{Qg}, $V_{\bar{Q}g}$, and V_{gg} respectively.

The equilibrium of the system at a constant temperature T is characterized by minimizing the grand potential A appropriate for the color-singlet Q and $\bar{Q}$ in dynamical motion in the quark-gluon plasma given by

$$\begin{aligned} A &= \mathcal{F}_1 - \mu(Q\bar{Q})N_{Q\bar{Q}} - \mu(g)N_g \\ &= \mathcal{U}_1 - T\mathcal{S}_1 - \mu(Q\bar{Q})N_{Q\bar{Q}} - \mu(g)N_g, \end{aligned} \tag{15}$$

where $\mathcal{F}_1$ is free energy, $\mathcal{U}_1$ the total internal energy, and $\mathcal{S}_1$ the total entropy for Q and $\bar{Q}$ in dynamical motion in the quark-gluon plasma. Only in their static limits when the heavy quark and antiquark are held spatially fixed can $\mathcal{F}_1, \mathcal{U}_1$, and $\mathcal{S}_1$ be equal to their corresponding static thermodynamical quantities F_1, U_1, and S_1. The quantities $\mu(Q\bar{Q})$ and $\mu(g)$ are the chemical potentials of Q-$\bar{Q}$ and gluons, respectively, and $N_{Q\bar{Q}}$ and N_g are the numbers of Q-$\bar{Q}$ and gluons respectively. Strictly speaking the number of gluons at thermal equilibrium depends on the length scale (the Q^2 value of the measuring probe) under consideration. In our schematic model, we can fix the length scale appropriate for Q-$\bar{Q}$ bound states in the quark-gluon plasma, and in that length scale the number of gluons, for the fixed spatial volume under consideration at thermal equilibrium at T, can be determined. We shall also ignore the annihilation of Q-$\bar{Q}$ into light quarks or photons and the corresponding inverse production so that the number of Q-$\bar{Q}$ pair can be considered fixed also. In Eq. (15), we need to add the Lagrange multipliers $\lambda_i(Q\bar{Q})$ and $\lambda_j(g)$ to the grand potential to constrain the normalization of the wave functions.

To carry out the minimization of the grand potential to obtain the equation of motion of the single-particle states, we can follow Bonche, Levit, and Vautherin [57–61] and write down the grand potential A explicitly. The internal energy $\mathcal{U}_1$ in Eq. (15) is $\mathcal{U}^{(1)}_{Q\bar{Q}} + \mathcal{U}^{(1)}_g - U_{g0}$, the sum of the internal energy of the heavy quark pair and the gluons, relative to the gluon internal energy when the heavy quark pair is not present. In terms of the wave function and occupation number degrees of freedom, the grand potential A can be written explicitly as

$$\begin{aligned} A = &\sum_i n_i(Q\bar{Q}) \int d\mathbf{r}\psi_i^\dagger(\mathbf{r}) \left[\frac{\hbar^2\mathbf{p}^2}{2\mu_{\rm red}} + V_{Q\bar{Q}}(\mathbf{r})\right]\psi_i(\mathbf{r}) \\ &+ \sum_{i,j} n_i(Q\bar{Q})n_j(g)\langle\psi_i\phi_j|V_{Qg} + V_{\bar{Q}g}|\psi_i\phi_j\rangle \\ &+ \sum_j n_j(g)\int d\mathbf{r}'\phi_j^\dagger(\mathbf{r}')\sqrt{\mathbf{p}_g^2 + m_{\rm eff}^2}\phi_j(\mathbf{r}') \\ &+ \sum_{j,k} n_j(g)n_k(g)\langle\phi_j\phi_k|V_{gg}|\phi_j\phi_k + \phi_k\phi_j\rangle/2 - U_{g0} \\ &+ T\sum_i [n_i(Q\bar{Q})\ln n_i(Q\bar{Q}) - \{1 + n_i(Q\bar{Q})\} \\ &\times \ln\{1 + n_i(Q\bar{Q})\}] + T\sum_j [n_j(g)\ln n_j(g) \\ &- \{1 + n_j(g)\}\ln\{1 + n_j(g)\}] \\ &- \mu(Q\bar{Q})\sum_i n_i(Q\bar{Q}) - \mu(g)\sum_j n_j(g) \\ &- \sum_i \lambda_i(Q\bar{Q})\langle\psi_i|\psi_i\rangle - \sum_j \lambda_j(g)\langle\phi_j|\phi_j\rangle. \end{aligned} \tag{16}$$

Here $\mathbf{p}$ and $\mu_{\rm red}$ are the relative momentum and the reduced mass of Q-$\bar{Q}$, $\mathbf{p}_g$ and $m_{\rm eff}$ are, respectively, the momentum and the effective mass of the gluon, and the dependence of various quantities on the temperature is made implicit. In this expression for the grand potential, the first two terms give $\mathcal{U}^{(1)}_{Q\bar{Q}}$, the third and fourth terms give $\mathcal{U}^{(1)}_g$, and the sixth and seventh terms give the entropy $T\mathcal{S}_1$. The matrix element $\langle\psi_i\phi_j|V_{Qg} + V_{\bar{Q}g}|\psi_i\phi_j\rangle$ is

$$\begin{aligned} \langle\psi_i\phi_j|V_{Qg} + V_{\bar{Q}g}|\psi_i\phi_j\rangle = &\int d\mathbf{r}d\mathbf{r}'\,\psi_i^\dagger(\mathbf{r})\phi_j^\dagger(\mathbf{r}')[V_{Qg}(\mathbf{r}' + \mathbf{r}/2) \\ &+ V_{\bar{Q}g}(\mathbf{r}' - \mathbf{r}/2)]\psi_i(\mathbf{r})\phi_j(\mathbf{r}'), \end{aligned} \tag{17}$$

and the matrix element $\langle\phi_j\phi_k|V_{gg}|\phi_j\phi_k + \phi_k\phi_j\rangle$ is

$$\begin{aligned} \langle\phi_j\phi_k|V_{gg}|\phi_j\phi_k + \phi_j\phi_k\rangle = &\int d\mathbf{r}'d\mathbf{r}''\,\phi_j^\dagger(\mathbf{r}')\phi_k^\dagger(\mathbf{r}'')V_{gg}(\mathbf{r}' - \mathbf{r}'') \\ &\times [\phi_j(\mathbf{r}')\phi_k(\mathbf{r}'') + \phi_k(\mathbf{r}')\phi_j(\mathbf{r}'')]. \end{aligned} \tag{18}$$

When we carry out the minimization of the grand potential with respect to the dynamical degrees of freedom, we obtain

five equations [Eqs. (24)–(28)]. By minimizing with respect to $\psi_i^\dagger(\mathbf{r})$, we obtain the equation of motion for $\psi_i(\mathbf{r})$ of the Q-$\bar{Q}$ system as

$$\left\{\frac{\hbar^2\mathbf{p}^2}{2\mu_{\rm red}} + V_1(\mathbf{r}, T) - \epsilon_i'(Q\bar{Q})\right\}\psi_i(\mathbf{r}) = 0, \tag{19}$$

where the color-singlet single-particle potential $V_1(\mathbf{r}, T)$ is

$$V_1(\mathbf{r}, T) = V_{Q\bar{Q}}(\mathbf{r}) + \sum_j n_j(g)\int d\mathbf{r}'\phi_j^\dagger(\mathbf{r}')[V_{Qg}(\mathbf{r}' + \mathbf{r}/2) + V_{\bar{Q}g}(\mathbf{r}' - \mathbf{r}/2)], \tag{20}$$

and $\epsilon_i'(Q\bar{Q}) = \lambda_i(Q\bar{Q})/n_i(Q\bar{Q})$. We note that in this equation, the quantity

$$\sum_j n_j(g)\phi_j^\dagger(\mathbf{r}')\phi_j(\mathbf{r}') = \rho_g(\mathbf{r}') \tag{21}$$

is the gluon density $\rho_g(\mathbf{r}')$. The color-singlet potential $V_1(\mathbf{r}, T)$ is

$$V_1(\mathbf{r}, T) = V_{Q\bar{Q}}(\mathbf{r}, T) + \int d\mathbf{r}'\rho_g(\mathbf{r}', T) \times [V_{Qg}(\mathbf{r}' + \mathbf{r}/2) + V_{\bar{Q}g}(\mathbf{r}' - \mathbf{r}/2)], \tag{22}$$

which represents the internal energy of a static color-singlet Q and $\bar{Q}$ at a separation $\mathbf{r}$ in the quark-gluon plasma. It has the same physical meaning as internal energy $U_{Q\bar{Q}}^{(1)}(\mathbf{r}, T)$ of a static color-singlet Q and $\bar{Q}$ at a separation $\mathbf{r}$ in the lattice gauge calculations. It is therefore reasonable to identify the Q-$\bar{Q}$ internal energy $U_{Q\bar{Q}}^{(1)}(\mathbf{r}, T)$ of the lattice gauge calculations as the single-particle potential $V_1(\mathbf{r}, T)$ in the Schrödinger equation (19) and write it as

$$\left\{\frac{\hbar^2\mathbf{p}^2}{2\mu_{\rm red}} + U_{Q\bar{Q}}^{(1)}(\mathbf{r}, T) - \epsilon_i'(Q\bar{Q})\right\}\psi_i(\mathbf{r}) = 0. \tag{23}$$

It is simplest to recalibrate the energy (and, similarly, the chemical potential) by $\epsilon_i(Q\bar{Q}) = \epsilon_i'(Q\bar{Q}) - U_{Q\bar{Q}}(\mathbf{r})_{r\to\infty}$ and rewrite this equation as

$$\left\{\frac{\hbar^2\mathbf{p}^2}{2\mu_{\rm red}} + U_{Q\bar{Q}}^{(1)}(\mathbf{r},T) - U_{Q\bar{Q}}^{(1)}(|\mathbf{r}| \to \infty, T) - \epsilon_i(Q\bar{Q})\right\}\psi_i(\mathbf{r}) = 0. \tag{24}$$

This Schrödinger equation involving $U_{Q\bar{Q}}^{(1)}(\mathbf{r}, T)$ is the proper equation of motion for quarkonium single-particle states.

From these considerations, the Q-$\bar{Q}$ potential in the equation of motion of quarkonium single-particle states is $U_{Q\bar{Q}}^{(1)}(\mathbf{r}, T)$. Lattice calculations so far provide information only on the free energy $F_1(\mathbf{r}, T)$ and the total internal energy $U_1(\mathbf{r}, T)$. It will be of great interest in future lattice work to evaluate $U_{Q\bar{Q}}^{(1)}(\mathbf{r}, T)$ so that it can be used as the proper Q-$\bar{Q}$ potential in quarkonium studies. In the next section, we shall present a method by which $U_{Q\bar{Q}}^{(1)}(\mathbf{r}, T)$ can be approximately evaluated by using the quark-gluon plasma equation of state.

The minimization of the grand potential with respect to the gluon wave function $\phi_j^\dagger(\mathbf{r})$ gives the equation of motion for the gluon states,

$$\left\{\sqrt{\mathbf{p}_g^2 + m_{\rm eff}^2} + \sum_i n_i(Q\bar{Q})\int d\mathbf{r}\psi_i^\dagger(\mathbf{r})[V_{Qg}(\mathbf{r}' + \mathbf{r}/2) + V_{\bar{Q}g}(\mathbf{r}' - \mathbf{r}/2)]\psi_i(\mathbf{r}) - \epsilon_i(g)\right\}\phi_j(\mathbf{r}') + \sum_k n_k(g) \times \int d\mathbf{r}''\phi_k^\dagger(\mathbf{r}'')V_{gg}(\mathbf{r}'' - \mathbf{r}')[\phi_k(\mathbf{r}'')\phi_j(\mathbf{r}') + \phi_k(\mathbf{r}')\phi_j(\mathbf{r}'')] + \sum_{\lambda,k} n_\lambda(g)n_k(g)\int d\mathbf{r}''\phi_\lambda^\dagger(\mathbf{r}')\phi_k^\dagger(\mathbf{r}'')\frac{\partial V_{gg}(\mathbf{r}'' - \mathbf{r}')}{\partial\rho_g} \times [\phi_k(\mathbf{r}'')\phi_\lambda(\mathbf{r}') + \phi_k(\mathbf{r}')\phi_\lambda(\mathbf{r}'')]n_j(g)\phi_j(\mathbf{r}') = 0, \tag{25}$$

where we have taken the density-dependent interaction as a delta function in $\mathbf{r}'' - \mathbf{r}'$ as in the Skyrme interaction [62, 63]. The minimization of the grand potential with respect to $n_i(Q\bar{Q})$ and $n_j(g)$ yields

$$n_i(Q\bar{Q}) = \frac{1}{e^{[\epsilon_i(Q\bar{Q}) - \mu(Q\bar{Q})]/T} - 1} \tag{26}$$

and

$$n_j(g) = \frac{1}{e^{[\epsilon_j(g) - \mu(g)]/T} - 1}, \tag{27}$$

which are the well-known Bose-Einstein distributions.

The variation of the grand potential A of Eq. (15) with respect to N_g gives

$$\partial A/\partial N_g = \mu(g).$$

The requirement that thermal equilibrium is reached when the variation of A with respect to N_g is a minimum leads to [64]

$$\mu(g) = 0. \tag{28}$$

The number of gluons at level j, $n_j(g)$, can then be obtained from Eq. (27) with $\mu(g) = 0$, and the total number of gluons N_g is given by

$$N_g = \sum_j n_j(g). \tag{29}$$

These considerations give a set of equations [Eqs. (24)–(28)] for a system in which both the quark-gluon plasma and the Q-$\bar{Q}$ are in thermal equilibrium. If a quarkonium is placed in a thermalized quark-gluon plasma for a period longer than the time needed for it to thermalize, the heavy quarkonium will reach thermal equilibrium and the Q-$\bar{Q}$ system will be described by this set of single-particle states with the Bose-Einstein distribution of occupation numbers.

Other cases of our interest are those in which the quark-gluon plasma has reached thermal equilibrium whereas the Q-$\bar{Q}$ system, which arises from the independent mechanism of nucleon-nucleon hard scattering, may not have. For such a case, the equations of motion for the gluon states and gluon occupation numbers, Eqs. (25) and (27), remain valid, except that in Eq. (25) the Q-$\bar{Q}$ occupation numbers $n_i(Q\bar{Q})$ will no longer obey the Bose-Einstein distribution (27). The equation of motion for the Q-$\bar{Q}$ single-particle states, Eq. (24), remains valid, as it depends on the gluon density. Because the heavy quark pair is a rare occurrence and gluons are

much greater in number, we expect that the gluon density and wave functions obtained in Eq. (25) are insensitive to the status of Q-$\bar{Q}$ thermalization, and they depend mainly on the thermalization of the gluons themselves. Therefore, single-particle states of the Q-$\bar{Q}$ system, $\psi_i(\mathbf{r})$, which depend on the gluon density as given by Eq. (23), are relatively insensitive to the thermalization status of Q-$\bar{Q}$, and they depend mainly on the thermalization status of the gluons.

In view of these considerations, the set of Q-$\bar{Q}$ single-particles states $\psi_i(\mathbf{r})$ of Eq. (24) can be used to examine the states of a Q-$\bar{Q}$ system, whether the Q-$\bar{Q}$ has reached thermal equilibrium or not. For example, one can introduce a bound Q-$\bar{Q}$ state ψ_λ into a thermalized quark-gluon plasma of temperature T. Such a system is described by a density matrix with an initial occupation number $n_i(Q\bar{Q}) = \delta_{i\lambda}$ at $t = 0$. The collision of the Q-$\bar{Q}$ with gluons in the medium will lead to the evolution of the occupation numbers of the Q-$\bar{Q}$ states as a function of time, leading eventually to the Bose-Einstein distribution characterized by the temperature of the medium.

The Q-$\bar{Q}$ system can exist in color-singlet and color-octet states. The consideration we have given can be generalized to color-octet states. The Schrödinger equation for the different single-particle color states a will depend on $U^{(a)}_{Q\bar{Q}}(\mathbf{r}, T)$. For the same reason that the Q-$\bar{Q}$ single-particle states depend on the thermalization status of the gluons and are insensitive to the thermalization status of Q-$\bar{Q}$, these single-particle states can be used to examine a Q-$\bar{Q}$ system in thermalized gluon matter. When the Q-$\bar{Q}$ also reaches thermal equilibrium, the set of states with occupation numbers given by Eqs. (26) will include both color-singlet and color-octet states.

VI. COLOR-SINGLET Q-$\bar{Q}$ POTENTIAL

From the variational principle of minimizing the grand potential, we find that the Schrödinger equation (24) contains the Q-$\bar{Q}$ internal energy $U^{(1)}_{Q\bar{Q}}$ as the quarkonium Q-$\bar{Q}$ potential. Lattice calculations so far provide information only on the free energy $F_1(\mathbf{r}, T)$ and the total internal energy $U_1(\mathbf{r})$, but not $U^{(1)}_{Q\bar{Q}}$. While we await accurate lattice gauge results for $U^{(1)}_{Q\bar{Q}}$, we can obtain an approximate $U^{(1)}_{Q\bar{Q}}$ from F_1 and U_1 by using the equation of state of the quark-gluon plasma and the first law of thermodynamics.

In the quenched approximation, the quark-gluon plasma consists of gluons only. We shall use the following strategy to obtain $U^{(1)}_{Q\bar{Q}}$. From lattice gauge calculations, we can calculate $F_1 - U_1$, which is equal to the entropy content TS_1 of the whole system. As the heavy quark Q and antiquark $\bar{Q}$ are held fixed in the lattice calculation, the entropy TS_1 comes entirely from the deconfined gluons, and it contains no contribution from the heavy quark Q-$\bar{Q}$ pair. From the entropy content of the gluon medium TS_1, we can deduce approximately the gluon internal energy $U^{(1)}_g$ by using the gluon medium equation of state and the first law of thermodynamics. Then, knowledge of the approximate gluon internal energy $U^{(1)}_g$ and the total internal energy U_1 gives a color-singlet potential $U^{(1)}_{Q\bar{Q}}$ in terms of F_1 and U_1.

Following such a strategy, we consider a deconfined gluon medium at temperature T with a static color-singlet Q and $\bar{Q}$ separated by a distance $\mathbf{r}$. We focus our attention on a volume element dV of gluons at spatial position $\mathbf{x}$ in which the gluon internal energy element is $dU^{(1)}_g$ and the gluon entropy element is dS_1. At this spatial location, a gluon experiences an external potential $\mathcal{V}(\mathbf{x})$ exerted by the color-singlet Q and $\bar{Q}$, other constituents, and induced charges. Hydrostatic equilibrium is reached when the local gluon pressure $p^{(1)}(\mathbf{x})$ at the volume element counterbalances the external forces. We can begin in the nonrelativistic description in which the total external force acting on a unit volume at $\mathbf{x}$ is $\rho_g(\mathbf{x})\nabla_{\mathbf{x}}\mathcal{V}(\mathbf{x})$ and hydrostatic equilibrium is reached when [65]

$$\nabla_{\mathbf{x}} p^{(1)}(\mathbf{x}) + \rho_g(\mathbf{x})\nabla_{\mathbf{x}}\mathcal{V}(\mathbf{x}) = 0. \tag{30}$$

In the relativistic case, one can describe the external interaction $\mathcal{V}(\mathbf{x})$ as part of the g^{00} metric, $g^{00} = 1 + 2\rho_g(\mathbf{x})\mathcal{V}(\mathbf{x})/\epsilon(\mathbf{x})$, and hydrostatic equilibrium is reached when [66,67]

$$\nabla_{\mathbf{x}} p^{(1)}(\mathbf{x}) + \{p^{(1)}(\mathbf{x}) + \epsilon^{(1)}_g(\mathbf{x})\}\nabla_{\mathbf{x}}\sqrt{1 + 2\rho_g(\mathbf{x})\mathcal{V}(\mathbf{x})/\epsilon^{(1)}_g(\mathbf{x})} = 0. \tag{31}$$

Thus, the external forces determine the gluon pressure $p^{(1)}(\mathbf{x})$ required to maintain hydrostatic equilibrium. At thermal equilibrium, the local gluon pressure is related to the local gluon entropy and the local gluon energy density. The external force therefore leads to a change of the gluon local entropy and the local gluon energy density.

According to this picture, the change in entropy is zero when the heavy quark sits on top of the heavy antiquark at $\mathbf{r} = 0$, because the color charges will neutralize for a color-singlet Q-$\bar{Q}$. As Q separates from $\bar{Q}$, the local gluon pressure, energy density, and entropy will increase in the vicinity of Q and $\bar{Q}$ to counterbalance the forces due to Q and $\bar{Q}$. The increase in entropy will reach a constant value at large separations when the Q and $\bar{Q}$ each independently causes a modification of the gluon distribution in its vicinity.

Under the temperature T and pressure $p^{(1)}(\mathbf{x})$, the gluon internal energy element $dU^{(1)}_g$ and the gluon entropy element dS_1 at $\mathbf{x}$ are related by the first Law of thermodynamics,

$$dU^{(1)}_g = T dS_1 - p^{(1)}(\mathbf{x}) dV, \tag{32}$$

where the superscript (1) denotes that the heavy quark Q-$\bar{Q}$ pair is in a color-singlet state. The local gluon internal energy density $\epsilon^{(1)}_g(\mathbf{x})$ is therefore related to the local gluon entropy density dS_1/dV and local gluon pressure $p^{(1)}(\mathbf{x})$ by

$$\epsilon^{(1)}_g(\mathbf{x}) = \frac{dU^{(1)}_g}{dV}(\mathbf{x}) = T\frac{dS_1}{dV}(\mathbf{x}) - p^{(1)}(\mathbf{x}). \tag{33}$$

The equation of state of a homogeneous quark-gluon plasma (gluon medium only in the case of the quenched approximation) has been obtained in previous lattice calculations [68]. It can be represented by expressing the ratio $p/(\epsilon/3)$ as a function $a(T)$ of temperature,

$$a(T) = \frac{p(T)}{\epsilon_g(T)/3}. \tag{34}$$

We shall make the local energy-density approximation in which the local gluon energy density $\epsilon^{(1)}_g(\mathbf{x})$ and the local gluon

pressure $p^{(1)}(\mathbf{x})$ under the temperature T obey the equation of state for the (homogeneous) bulk quark-gluon plasma so that

$$\frac{p^{(1)}(\mathbf{x})}{\epsilon_g^{(1)}(\mathbf{x})/3} = a(T), \tag{35}$$

as in the usual hydrodynamical description of the quark-gluon plasma. We then have

$$\frac{dU_g^{(1)}}{dV}(\mathbf{x}) = \frac{3}{3+a(T)}\frac{TdS_1}{dV}(\mathbf{x}). \tag{36}$$

When we integrate the local gluon energy density over the whole volume of $\mathbf{x}$ under consideration, we obtain

$$U_g^{(1)}(\mathbf{r},T) = \int d\mathbf{x}\frac{dU_g^{(1)}}{dV}(\mathbf{x}) = \frac{3}{3+a(T)}\int d\mathbf{x}\frac{TdS_1}{dV}(\mathbf{x}) = \frac{3}{3+a(T)}TS_1(\mathbf{r},T). \tag{37}$$

In a lattice gauge calculation, the large degrees of freedom of the gauge field and the maintenance of a thermal bath of constant temperature T make it reasonable to assume local thermal equilibrium and use the equation of state of homogeneous bulk matter to relate the local energy density to the local pressure in the local energy-density approximation. It will be of great interest to check Eq. (37) in future lattice gauge calculations to test the validity of the local energy-density approximation.

For the case in the absence of the Q-$\bar{Q}$ pair, the gluon internal energy $U_{g0}(T)$ and the gluon entropy $S_0(T)$ are similarly related by

$$U_{g0}(T) = \frac{3}{3+a(T)}TS_0(T). \tag{38}$$

We therefore have

$$U_g^{(1)}(\mathbf{r},T) - U_{g0}(T) = \frac{3}{3+a(T)}T\left\{S_1(\mathbf{r},T) - S_0(T)\right\}. \tag{39}$$

In the previous discussions from Eq. (32) to Eq. (39), we have followed the standard practice of using the convention of "absolute" units in which the entropy S_1(absolute) and S_0(absolute) are measured relative to zero entropy. However, in lattice calculations and in Sec. IV, we have used the "lattice gauge calculation" convention in which the entropy S_1(lattice) and the free energy F_1(lattice) with the Q-$\bar{Q}$ pair are measured relative, respectively, to the entropy S_0(absolute) and free energy F_0(absolute) without the Q-$\bar{Q}$ pair [i.e., S_1(lattice) = S_1(absolute) − S_0(absolute) and F_1(lattice) = F_1(absolute) − F_0(absolute)]. Henceforth, we shall switch back to the "lattice gauge calculation" convention in which the entropy $S_1(\mathbf{r},T)$ and the free energy $F_1(\mathbf{r},T)$ with the Q-$\bar{Q}$ pair are measured relative to those in the absence of the Q-$\bar{Q}$ pair. In this lattice gauge convention, Eq. (39) can be rewritten as

$$U_g^{(1)}(\mathbf{r},T) - U_{g0}(T) = \frac{3}{3+a(T)}TS_1(\mathbf{r},T). \tag{40}$$

Using the relation $TS_1 = U_1 - F_1$ of Eq. (10) in lattice gauge theory, we can express $U_g^{(1)}(\mathbf{r},T) - U_{g0}(T)$ in terms of $F_1(\mathbf{r},T)$ and $U_1(\mathbf{r},T)$ as follows:

$$U_g^{(1)}(\mathbf{r},T) - U_{g0}(T) = \frac{3}{3+a(T)}\{U_1(\mathbf{r},T) - F_1(\mathbf{r},T)\}. \tag{41}$$

Substituting this equation in Eq. (11), we obtain

$$U_{Q\bar{Q}}^{(1)}(\mathbf{r},T) = \frac{3}{3+a(T)}F_1(\mathbf{r},T) + \frac{a(T)}{3+a(T)}U_1(\mathbf{r},T). \tag{42}$$

The Q-$\bar{Q}$ potential that appears in the Schrödinger equation for quarkonium bound states, Eq. (24), is then

$$\begin{aligned} U_{Q\bar{Q}}^{(1)}(\mathbf{r},T) - U_{Q\bar{Q}}^{(1)}(\mathbf{r}\to\infty,T) &= f_F(T)\left\{F_1(\mathbf{r},T) - F_1(\mathbf{r}\to\infty,T)\right\} \\ &\quad + f_U(T)\left\{U_1(\mathbf{r},T) - U_1(\mathbf{r}\to\infty,T)\right\}, \end{aligned} \tag{43}$$

where

$$f_F(T) = \frac{3}{3+a(T)}, \tag{44}$$

$$f_U(T) = \frac{a(T)}{3+a(T)}, \tag{45}$$

and $f_F(T) + f_F(T) = 1$. We shall use such a relation to obtain an approximate Q-$\bar{Q}$ potential from F_1 and U_1.

Equation (43) has been obtained for a color-singlet Q-$\bar{Q}$ pair in the quenched approximation. It can be easily generalized to the case of the unquenched full QCD with dynamical light quarks. In that case, the function $a(T)$ corresponds to the $p/(\epsilon/3)$ appropriate for the equation of state of the quark-gluon plasma under consideration, $U_{g0}(T)$ of Eq. (42) becomes $U_{qgp}(T)$, the internal energy of the quark-gluon plasma in the absence of the Q-$\bar{Q}$ pair, and Eq. (43) remains unchanged.

We show ϵ/T^4 and p/T^4 obtained in quenched QCD by Boyd *et al.* [68] as a function of T/T_c in Fig. 1(a). In Fig. 1(b) the function $a(T)$, defined as the ratio $3p/\epsilon$, is plotted as a function of T/T_c. The free energy fraction

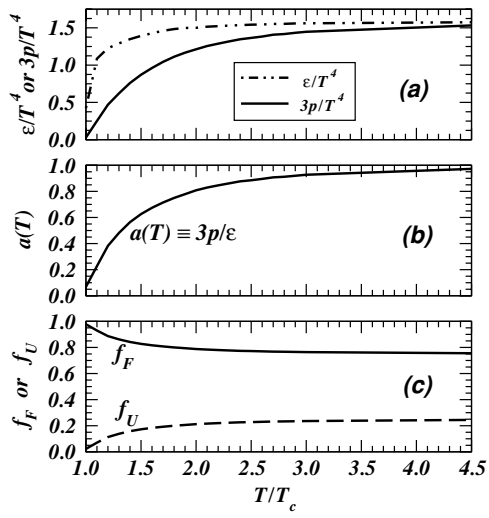

FIG. 1. (a) The energy density and pressure of a SU(3) gauge theory as a function of the temperature obtained by Boyd *et al.* [68]. (b) The ratio of $3p/\epsilon$ as a function of T/T_c. (3) The weight f_F of F_1 and the weight f_U of U_1 that comprise the Q-$\bar{Q}$ potential according to Eq. (43).

$f_F(T)$ and the internal energy fraction $f_U(T)$ calculated using this ratio of $a(T)$ are shown in Fig. 1(c). One finds that at temperatures close to T_c, f_F is close to unity, and the Q-$\bar{Q}$ potential is close to the free energy $F_1(\mathbf{r})$. As temperature increases, the F_1 fraction decreases but approaches $f_F \sim 0.75$ at very high temperatures. The U_1 fraction is nearly zero at temperatures near T_c and it increases monotonically as a function of temperature, reaching a value of 0.25 at very high temperatures.

It is of interest to discuss the conditions under which the application of the static potential $U^{(1)}_{Q\bar{Q}}(\mathbf{r}, T)$ and its representation in terms of F_1 and U_1 as given in Eq. (43) can be reasonable concepts. For the static potential and the quark-gluon plasma equation of state to be applicable, the time for the quark-gluon plasma to reach thermal and hydrostatic equilibrium must be short compared with the time for the periodic motion of the Q and $\bar{Q}$. The time for the quark-gluon plasma to reach thermal equilibrium is of the order 0.6 fm/c, as one may infer from the discussion in Sec. II. The orbiting time for a heavy quarkonium is of order $2r_{\rm rms}/v$, where $r_{\rm rms}$ is the root-mean-square radius of the heavy quarkonium system and v is the relative velocity, which is at most of order 0.5 for heavy quarks. The spatial scale of the heavy quarkonia in the quark gluon plasma is quite large. As we shall see in Secs. VIII and IX $r_{\rm rms} = 0.88$ fm at $T/T_c = 1.13$ for J/ψ and it increases to $r_{\rm rms} = 5.3$ fm at $T/T_c = 1.65$. For Υ, $r_{\rm rms} = 0.25$ fm at $T/T_c = 1.13$ and it increases to $r_{\rm rms} = 0.59$ fm at $T/T_c = 2.6$. The large spatial scales arises because these heavy quarkonium states are basically only weakly bound. The orbiting time for heavy quarkonia in the quark-gluon plasma is much greater than the quark-gluon plasma thermalization time. It is therefore reasonable to use a static Q-$\bar{Q}$ potential and the equation of state of the quark-gluon plasma to study heavy quarkonium in the quark-gluon plasma.

VII. SIMPLE PARAMETRIZATIONS OF U_1 AND F_1

Kaczmarek *et al.* [22] obtained the color-singlet free energy $F_1(\mathbf{r}, T)$ and internal potential $U_1(\mathbf{r}, T)$ in quenched QCD as a function of $r = |\mathbf{r}|$ and T. The radial dependences of $F_1(\mathbf{r}, T)$ and $U_1(\mathbf{r}, T)$ in quenched QCD can be adequately represented by a screened Coulomb potential with a screening mass μ_i, a coupling constant α_i, and an asymptotic potential horizon $C_i(T)$ at $|\mathbf{r}| \to \infty$, where the subscript $i = F$ and U stands for the free energy or the internal energy, respectively:

$$F_1(\mathbf{r}, T) = C_F(T) - \frac{4\alpha_F(T)}{3}\frac{e^{-\mu_F r}}{r} \tag{46}$$

and

$$U_1(\mathbf{r}, T) = C_U(T) - \frac{4\alpha_U(T)}{3}\frac{e^{-\mu_U r}}{r}. \tag{47}$$

The parameters C_i, α_i, and μ_i for the quenched lattice QCD results of $F_1(\mathbf{r}, T)$ and $U_1(\mathbf{r}, T)$ of Kaczmarek *et al.* [22] are shown in Figs. 2 and 3, and the corresponding fits to the lattice F_1 and U_1 results are shown in Figs. 4 and 5. The coupling constant $\alpha_F(T)$ is 0.44 at $T = 1.05T_c$. As the temperature increases, α_F decreases and saturates at $\alpha_F \sim 0.3$ at $T \sim 3T_c$.

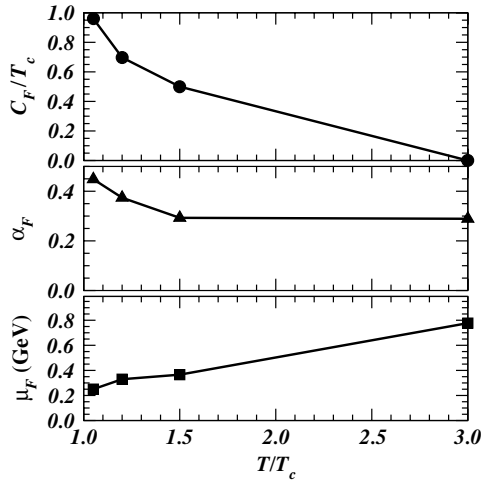

FIG. 2. The color-singlet parameters C_F, α_F, and μ_F for the free energy $F_1(\mathbf{r}, T)$ as given in Eq. (46).

The screening mass μ_F is about 0.25 GeV at temperatures just above T_c and it increases to 0.8 GeV at $3T_c$.

The coupling constant $\alpha_U(T)$ is quite large at temperatures slightly above the phase-transition temperature. At $T = 1.13T_c$, $\alpha_U = 1.26$. As the temperature increases, α_U decreases and saturates at $\alpha_U(T) \sim 0.4$ at $T \sim 4T_c$. The screening mass μ_U is small at temperatures just above T_c. As the temperature increases, the screening mass μ_U increases to about 0.8 GeV at $T \sim 4.5T_c$.

The comparison in Figs. 4 and 5 shows that the free energy F_1 and the internal energy U_1 with the set of parameters in Figs. 2 and 3 adequately describe the lattice gauge data and can be used to calculate the eigenvalues and eigenfunctions of heavy quarkonia. In the local energy-density approximation, the Q-$\bar{Q}$ potential is given by

$$U^{(1)}_{Q\bar{Q}}(\mathbf{r}, T) - U^{(1)}_{Q\bar{Q}}(\mathbf{r} \to \infty, T) = -\frac{4}{3}\frac{f_F(T)\alpha_F(T)e^{-\mu_F r} + f_U(T)\alpha_U(T)e^{-\mu_U r}}{r}. \tag{48}$$

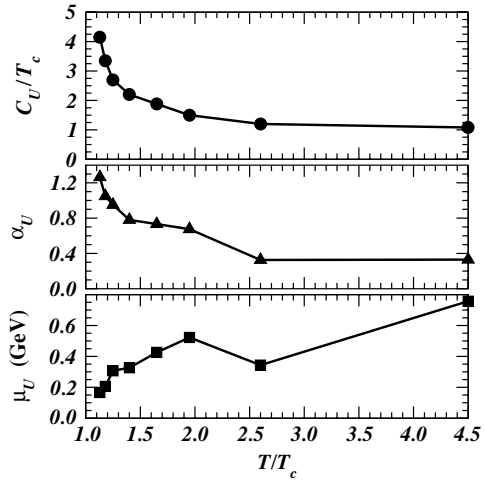

FIG. 3. The color-singlet parameters C_U, α_U, and μ_U for the total internal energy $U_1(\mathbf{r}, T)$ as given in Eq. (47).

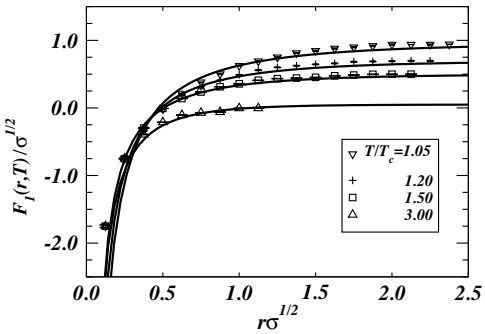

FIG. 4. The symbols represent the quenched lattice QCD free energy, $F_1(r, T)/\sigma^{1/2}$, of Kaczmarek *et al*. [22] at selected distances and the curves are the fits using the screened Coulomb potential, Eq. (46), with parameters given in Fig. 2. Here $\sigma^{1/2} = 425$ MeV.

VIII. CHARMONIUM IN THE QUARK-GLUON PLASMA

In the quenched approximation, the transition temperature is $T_c = 269$ MeV [8]. To evaluate the energy levels of different heavy quarkonia, we use this value of T_c to express the potential in GeV units.

For a given temperature, we use the $U^{(1)}_{Q\bar{Q}}(\mathbf{r}, T)$ potential given in Eq. (43) to calculate the charmonium energy levels and wave functions. In these calculations, we employ charm quark masses $m_c = 1.3$ and 1.5 GeV [69] to provide an indication of the uncertainties of the eigenenergies.

Energy levels of charmonium calculated with the $U^{(1)}_{Q\bar{Q}}(\mathbf{r}, T)$ potential are shown in Fig. 6 as a function of temperature. The J/ψ and η_c states are weakly bound at temperatures slightly greater than T_c. The eigenenergies of J/ψ and η_c are -0.045 GeV at $T = 1.13T_c$ for $m_c = 1.5$ GeV and their energies increase as the temperature increases. The J/ψ and η_c state eigenenergies are -0.0004 GeV at $T = 1.65T_c$ for $m_c = 1.5$ GeV. If one extrapolates the eigenenergy from lower temperature points, one infers that the J/ψ and η_c spontaneous dissociation temperature is $1.52T_c$ for $m_c = 1.3$ GeV and is $1.72T_c$ for $m_c = 1.5$ GeV, with a mean value of $1.62T_c$. There are no bound χ_c, ψ', and η'_c states for temperatures above T_c.

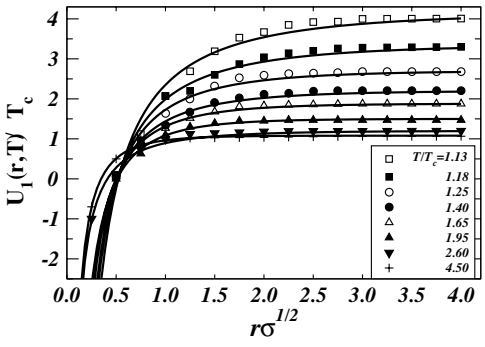

FIG. 5. The symbols represent the quenched lattice QCD total internal energy, $U_1(r, T)/T_c$, of Kaczmarek *et al*. [22] at selected distances and the curves are the fits using the screened Coulomb potential, Eq. (47), with parameters given in Fig. 3. Here $T_c = 269$ MeV and $\sigma^{1/2} = 425$ MeV.

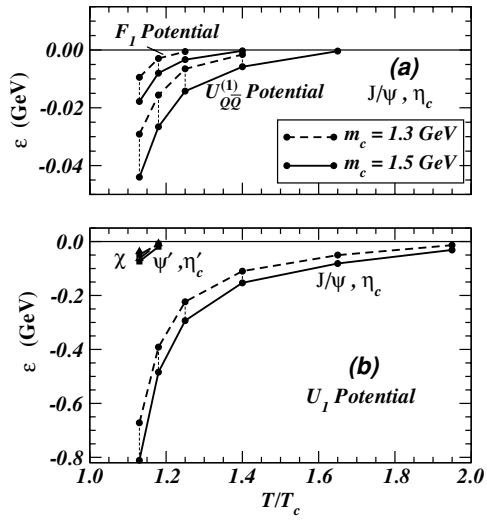

FIG. 6. Energy levels of charmonium in the quark-gluon plasma as a function of temperature calculated with (a) the $F_1(\mathbf{r}, T)$ and $U^{(1)}_{Q\bar{Q}}(\mathbf{r}, T)$ potentials for J/ψ and η_c, and (b) the $U_1(\mathbf{r}, T)$ potential for J/ψ, η_c, χ_c, ψ', and η'_c. The dashed curves are obtained with $m_c = 1.3$ GeV and the solid curves with $m_c = 1.5$ GeV. Note the difference in the enegy scales in (a) and (b).

In the spectral function analyses of Asakawa *et al*. [9,10] and Petreczky *et al*. [11–13], the widths of J/ψ begin to be broadened at $\sim 1.6T_c$ and the χ_c states are found to be dissolved already at $1.13T_c$. The width of J/ψ can be broadened by gluon dissociation $g + J/\psi \to c + \bar{c}$, which is presumably a possible process in the lattice gauge calculations in the spectral function analysis. The gluon dissociation width is however of the order of 0.05–0.1 GeV as one can infer later from Sec. XII. In the numerical results of the spectral function analysis [9,10], the width appears to be broadened by an amount significantly greater than this amount for gluon dissociation. It is therefore reasonable to associate the broadening of the width of a heavy quarkonium in the spectral function analysis with the occurrence of spontaneous dissociation, when the heavy quarkonium becomes unbound. The temperature at which the width of a quarkonium begins to broaden significantly can be taken as the dissociation temperature for spontaneous dissociation of the quarkonium in the spectral function analysis.

In Table I we list the dissociation temperatures of different quarkonia obtained in quenched QCD. A comparison of the dissociation temperatures from the spectral function analysis [9–13] and from the $U^{(1)}_{Q\bar{Q}}(\mathbf{r}, T)$ potential model indicates the agreement that J/ψ is bound up to about $1.6T_c$ and is unstable at very high temperatures. There is also the agreement that the χ_c and ψ' states are unbound in the quark-gluon plasma.

It is instructive to compare the eigenenergies obtained by using other potential models. We calculate the heavy quarkonium eigenenergies with the $F_1(\mathbf{r}, T)$ potential as in Refs. [25–28] by replacing $U^{(1)}_{Q\bar{Q}}$ in Eq. (24) with $F_1(\mathbf{r}, T)$. In Fig. 6(a), we show the charmonium energies calculated with the $F_1(\mathbf{r}, T)$ potential. One finds that J/ψ is weakly bound, but the dissociation temperature lies in the range 1.33–$1.46T_c$

TABLE I. Dissociation temperatures obtained from different analyses in quenched QCD.

Heavy quarkonium	$U^{(1)}_{Q\bar{Q}}(\mathbf{r}, T)$ potential	$F_1(\mathbf{r}, T)$ potential	$U_1(\mathbf{r}, T)$ potential	Spectral analysis
J/ψ, η_c	$1.62T_c$	$1.40T_c$	$2.60T_c$	$\sim 1.6T_c$
χ_c	unbound in QGP	unbound in QGP	$1.19T_c$	dissolved below $1.1T_c$
ψ', η_c'	unbound in QGP	unbound in QGP	$1.20T_c$	
Υ, η_b	$4.10T_c$	$3.50T_c$	$\sim 5.0T_c$	
χ_b	$1.18T_c$	$1.10T_c$	$1.73T_c$	
Υ', η_b'	$1.38T_c$	$1.19T_c$	$2.28\,T_c$	

for $m_c = 1.3$–1.5 GeV, with a mean value of $1.40T_c$. This dissociation temperature is lower than that inferred from the spectral function analysis. The χ_c and ψ' states are unbound in this potential.

We also calculate the heavy quarkonium eigenenergies with the total internal energy $U_1(\mathbf{r}, T)$ as the Q-$\bar{Q}$ potential as in Refs. [25–28]. The eigenenergies for charmonium states are shown in Fig. 6(b). Because the total internal energy U_1 contains a deeper potential well, the charmonium states are deeply bound. The binding energy is about 0.8 GeV at $1.13T_c$, and the state becomes unbound at 2.50–$2.71T_c$, with a mean value of $2.60T_c$. This dissociation temperature is much higher than the dissociation temperature of about $1.6T_c$ obtained from the spectral function analysis. There are uncertainties in the spontaneous dissociation temperatures owing to the differences in the degrees of freedom assumed in lattice QCD calculations. For example, using the total internal energy U_1 extracted from the full QCD with two flavors obtained by Kaczmarek *et al.* [70], Shuryak found that the dissociation temperature of J/ψ is about $2.7T_c$ [15]. In this model, the χ_c, ψ', and η_c' states are bound at temperature slightly above T_c and they become unbound at $1.2T_c$. The binding of χ_c states is in disagreement with the results of the dissolution of χ_c states in the spectral function analysis.

Our comparison of these results indicate that the model that compares best with the spectral function analysis is the $U^{(1)}_{Q\bar{Q}}(\mathbf{r}, T)$ potential [Eq. (43)] obtained from a variational principle and the quark-gluon plasma equation of state. However, as the results from the spectral function analysis are still scanty, more results from the spectral function analysis are needed to test further the potential model.

The solution of the Schrödinger equation (19) gives both eigenenergies and eigenfunctions. We show in Fig. 7 the wave functions of J/ψ calculated with the $U^{(1)}_{Q\bar{Q}}$ potential and $m_c = 1.5$ GeV. They are normalized according to

$$\int_0^\infty |u_{1S}(r)|^2 dr = \int_0^\infty |r\psi_{1S}(r)|^2 dr = 1, \qquad (49)$$

as in Eq. (4.18) of Blatt and Weisskopf [71]. As the temperature increases, the binding of the state becomes weaker and the wave function extends to greater distances. The rms r of the J/ψ wave function is 0.88 fm at $1.13T_c$. At $T = 1.65T_c$, which is near the temperature for spontaneous dissociation, the binding energy is 0.0004 GeV. The rms r of the J/ψ wave function is 5.30 fm, which is much greater than the theoretical rms r of 0.404 fm for J/ψ at zero temperature [72].

IX. BOTTOMIUM BOUND STATES IN THE QUARK-GLUON PLASMA

One can carry out similar calculations for the energy levels and wave functions of the b-$\bar{b}$ system. We take the mass of the bottom quark to be 4.3 GeV, which falls within the range of 4.1–4.5 GeV in the PDG listing [69]. The energy levels of the lowest b-$\bar{b}$ bound states calculated with the $U^{(1)}_{Q\bar{Q}}(\mathbf{r}, T)$ potential are shown in Fig. 8 as a function of temperature. We find that at $T = 1.13T_c$, the Υ state lies at about -0.3 GeV and the state energy increases as the temperature increases. The Υ state remains bound by 0.028 GeV at $T = 2.5T_c$. If one extrapolates from lower temperatures, the dissociation temperature of Υ and η_b is $4.10T_c$. For this potential, the χ_b, Υ', and η_b' states are weakly bound at temperatures slightly greater than T_c. The χ_b states become unbound at $1.18T_c$ and the Υ' and η_b' become unbound at $1.38T_c$.

As a comparison, we calculate the bottomium eigenenergies using other potential models. If we assume that the Q-$\bar{Q}$ potential is the free energy, $F_1(\mathbf{r}, T)$, we find that Υ is bound by about 0.2 GeV at $1.13T_c$ and it becomes unbound at $3.50T_c$, as shown in Fig. 9(a). The χ_b states are unbound at $1.10T_c$, and the Υ' and η_b' states are bound by 0.003 GeV at $1.13T_c$, which should be close to its dissociation temperature.

If we assume that the Q-$\bar{Q}$ potential is the total internal energy, $U_1(\mathbf{r}, T)$, we find that the bottomium states become deeply bound, as shown in Fig. 9(b). At $1.13\ T_c$, the Υ and η_b states are bound by about 3 GeV. The binding energy decreases slowly as a function of temperature. The small binding energy at $T = 4.5T_c$ indicates that the Υ dissociation temperature is close to and slightly greater than $T \sim 5.0T_c$. Because of the

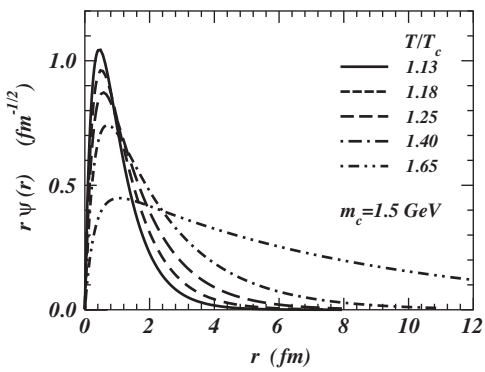

FIG. 7. J/ψ wave function calculated with the $U^{(1)}_{Q\bar{Q}}(\mathbf{r}, T)$ potential for different temperatures.

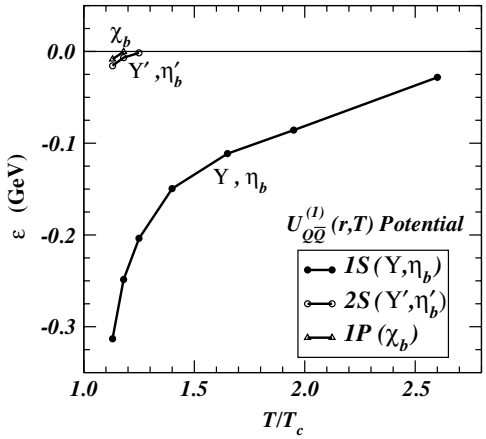

FIG. 8. Energy levels of b-$\bar{b}$ bound states as a function of temperature, calculated with the $U^{(1)}_{Q\bar{Q}}(\mathbf{r}, T)$ potential.

small screening mass near T_c, the potential for temperatures near T_c is approximately a Coulomb potential but with a large coupling constant. Hence, χ_b and Υ', η'_b states are nearly degenerate. They lie at -0.5 GeV for $T = 1.13T_c$ and begin to be unbound at $1.73T_c$ and $2.28T_c$, respectively.

The b-$\bar{b}$ bound state wave functions can be obtained by solving the Schrödinger equation (19). We show in Fig. 10 the Υ radial wave functions as a function of temperature. The wave function extends to greater distances as the temperature increases. The root-mean-square radius $r_{\rm rms}$ is 0.25 fm at $T/T_c = 1.13$ and it increases as the temperature increases. At $T = 2.6T_c$, which lies very close to the temperature for spontaneous dissociation, the rms r value is 0.59 fm, which is substantially greater than the rms r of 0.25 fm at $1.13T_c$.

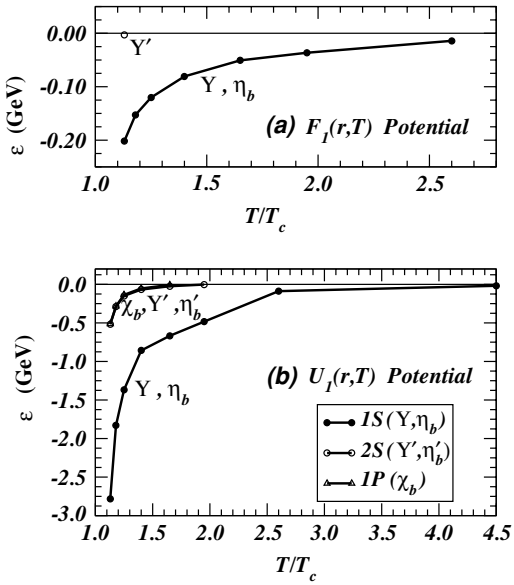

FIG. 9. Energy levels of b-$\bar{b}$ bound states as a function of temperature calculated with (a) the $F_1(\mathbf{r}, T)$ potential and (b) the $U_1(\mathbf{r}, T)$ potential.

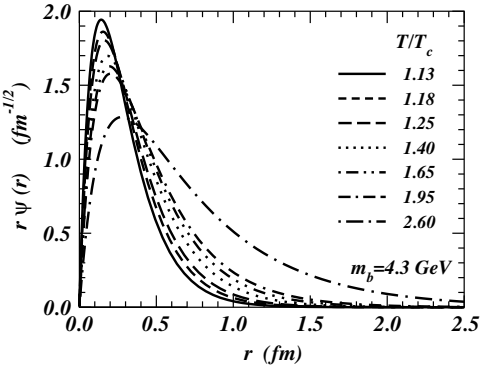

FIG. 10. Υ wave function $r\psi(r)$ as a function of temperature.

Our comparisons of the charmonium eigenenergies with those from the spectral function analysis indicate that the results obtained by using the $U^{(1)}_{Q\bar{Q}}$ potential agree best with the spectral function analysis. As different models give different predications on the bottomium dissociation temperatures, further tests of the models can be carried out by calculating the dissociation temperature of bottomium states using the spectral function analysis.

X. ANTISCREENING BY DECONFINED GLUONS

As one crosses the phase-transition temperature T_c from below, quarks and gluons becomes deconfined. The Debye screening resulting from the interaction between the heavy quark and antiquark with medium particles is considered to be the dominant effect when a heavy quarkonium is placed in a quark-gluon plasma [1]. It is argued that Debye screening leads to a decrease in the attractive interaction between the heavy quark and antiquark and results in the spontaneous dissociation of the heavy quarkonium in the quark-gluon plasma. The suppression of J/ψ production was suggested as a signature for the quark-gluon plasma [1].

In perturbative QCD, there is a relation between the screening mass μ, coupling constant $g = \sqrt{4\pi\alpha_s}$, and temperature T in a quark-gluon plasma given by [73–77]

$$\mu^2 = g^2T^2(N_c + N_f/2)/3. \tag{50}$$

For the quenched approximation with $N_f = 0$, perturbative QCD gives $\mu = gT$. A comparison of the effective coupling constants α_F and α_U of either F_1 or U_1 with the screening mass μ_F and μ_U at temperatures near T_c indicates that the screening mass is much smaller than the estimates in the perturbative QCD limit, indicating that the large-distance behavior cannot be qualitatively described by perturbative QCD. The perturbative QCD limit for the large-distance behavior can be reached only at temperatures above $6T_c$ [78,79]. In fact, Kaczmarek *et al.* [79] pointed out that for temperatures close to T_c the QCD phase should be more appropriately described in terms of remnants of the confinement part of QCD rather than a strongly coupled Coloumbic force [14,15]. To understand this "remnant of QCD confinement above T_c," it is of interest to examine the effects of antiscreening above T_c by deconfined gluons.

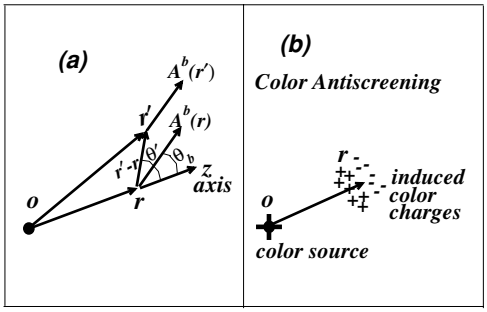

FIG. 11. (a) The coordinate system used in the evaluation of the induced color charge density $\rho^{\lambda(2)}_{\rm ind}(\mathbf{r}', \mathbf{r})$ at $\mathbf{r}'$. (b) A heavy quark of color source at O induces color charges of the same sign in the direction forward of $\mathbf{r}$ and color charges of the opposite sign in the direction backward of $\mathbf{r}$.

In a related topic, Svetitsky, Yaffe, DeTar, and DeGrand previously found that large spacelike Wilson loops in the quark-gluon plasma have an area law behavior [2,3,31,33,34]. As the area law of the spatial Polyakov loop does not change drastically across the phase transition, DeTar [2,3], Hansson, Lee, and Zahed [4], and Simonov [5–7] argued that low-lying mesons including J/ψ may remain in relatively narrow states owing to the attractive interaction between the quark and the antiquark and that the suppression of J/ψ is not a signature of the deconfinement phase transition [3]. It is of interest to examine the consequence of the spatial area law to see whether it will lead to antiscreening between a heavy quark and antiquark.

The mechanism of antiscreening by virtual gluons at $T = 0$ is well known (see, for example, Peskin and Schroeder, Gottfried and Weisskopf [80] and [81]). We follow similar arguments to study the mechanism of antiscreening by deconfined gluons above the phase-transition temperature T_c. We consider the color electric field generated by a static color source $\rho^{a(0)}_{\rm ext}(\mathbf{r}) = \delta(\mathbf{r})\delta^{a\lambda}$ with a unit color charge of index λ placed at the origin, in the presence of an external gauge field [Fig. 11(a)]. We fix the gauge to be the Coulomb gauge and represent the deconfined gluons in terms of an external transverse gluon field $A^{bi}(\mathbf{r})$, where the first index $b = 1, \ldots, 8$ is the color index and the second index $i = 1, 2, 3$ is the spatial coordinate index.

The color electric field $E^{ai}(\mathbf{r})$ generated by the source is determined by the Gauss law

$$\partial_i E^{ai}(\mathbf{r}) = g\delta(\mathbf{r})\delta^{a\lambda} + g f^{abc} A^{bi}(\mathbf{r}) E^{ci}(\mathbf{r}) \qquad (51)$$

(Eq. (16.139) of Peskin and Schroeder [81]). Here repeated indices are summed over and the first index of $E^{ai}(\mathbf{r})$ is the color index and the second index is the spatial coordinate index. Because of the nonlinear nature of the second term, which arises from the non-Abelian nature of QCD, the external color source $\delta(\mathbf{r})\delta^{a\lambda}$ and the external gauge field $A^{ai}(\mathbf{r})$ induce a color source $\rho^{a(1)}_{\rm ind}(\mathbf{r})$, which in turn induces an additional color source $\rho^{a(2)}_{\rm ind}(\mathbf{r})$. How do these induced color charges depend on the external gauge field $A^{bi}(\mathbf{r})$?

We consider an expansion of the source in terms of the external source and the induced sources, in powers of the coupling constant

$$\partial_i E^{ai}(\mathbf{r}) = g\delta(\mathbf{x})\delta^{a1} + g\rho^{a(1)}_{\rm ind}(\mathbf{r}) + g\rho^{a(2)}_{\rm ind}(\mathbf{r}) + \cdots. \qquad (52)$$

In the Coulomb gauge, the color field $E^{ci(1)}(\mathbf{r})$, arising only from the external static source $\delta(\mathbf{r})\delta^{a\lambda}$, is

$$E^{ai(1)}(\mathbf{r}) = g\delta^{a\lambda}\frac{r^i}{r^3}. \qquad (53)$$

From the nonlinear term in Eq. (51), the color charge density induced at $\mathbf{r}$ by the external gauge field $A^{\beta i}(\mathbf{r})$ and the electric field $E^{ci(1)}(\mathbf{r})$ of the external color source is

$$\rho^{a(1)}_{\rm ind}(\mathbf{r}) = f^{a\beta\gamma} A^{\beta i}(\mathbf{r}) E^{\gamma i(1)}(\mathbf{r}) = g f^{a\beta\gamma} A^{\beta i}(\mathbf{r}) \frac{\delta^{\gamma\lambda} r^i}{r^3}. \qquad (54)$$

An induced color-charge element $\rho^{a(1)}_{\rm ind}(\mathbf{r})\Delta\mathbf{r}$ at $\mathbf{r}$ will generate a field $E^{ai(2)}(\mathbf{r}', \mathbf{r})$ at $\mathbf{r}'$ and this field is pointing along the direction of $\mathbf{r}' - \mathbf{r}$,

$$E^{ai(2)}(\mathbf{r}', \mathbf{r}) = g\left[\rho^{a(1)}_{\rm ind}(\mathbf{r})\Delta\mathbf{r}\right]\frac{(r'^i - r^i)}{|\mathbf{r}' - \mathbf{r}|^3}. \qquad (55)$$

From the nonlinear term in Eq. (51), the color charge density element $\rho^{a(2)}_{\rm ind}(\mathbf{r}', \mathbf{r})\Delta\mathbf{r}$, which is induced at $\mathbf{r}'$ by the external gauge field $A^{bi}(\mathbf{r}')$ and the electric field $E^{ci(2)}(\mathbf{r}', \mathbf{r})$ at $\mathbf{r}'$, is therefore

$$\begin{aligned}
&\rho^{a(2)}_{\rm ind}(\mathbf{r}', \mathbf{r})\Delta\mathbf{r} \\
&\quad = f^{abc} A^{bi}(\mathbf{r}') E^{ci(2)}(\mathbf{r}', \mathbf{r}) \\
&\quad = g^2 f^{abc} A^{bi}(\mathbf{r}') \left[f^{c\beta\gamma} A^{\beta j}(\mathbf{r}) \frac{\delta^{\gamma\lambda} r^j}{|\mathbf{r}|^3} \Delta\mathbf{r} \right] \frac{(r'^i - r^i)}{|\mathbf{r}' - \mathbf{r}|^3}. \qquad (56)
\end{aligned}$$

Because the external source has the color index λ, we would like to study the induced color charge of index λ to see whether the induced color charges lead to screening or antiscreening. From Eq. (54), we have

$$\rho^{\lambda(1)}_{\rm ind}(\mathbf{r}) = 0, \qquad (57)$$

as $f^{\lambda\beta\lambda} = 0$ on account of the antisymmetric property of f. For the next-order induced color charge density element $\rho^{a(2)}_{\rm ind}(\mathbf{r}', \mathbf{r})\Delta\mathbf{r}$, we can write out explicitly the summations of color and spatial indices of Eq. (56),

$$\begin{aligned}
\rho^{\lambda(2)}_{\rm ind}(\mathbf{r}', \mathbf{r})\Delta\mathbf{r} = g^2 &\sum_{b,c,\beta=1}^{8} f^{\lambda bc} f^{c\beta\lambda} \\
&\times \sum_{i,j=1}^{3} \frac{A^{bi}(\mathbf{r}')(r'^i - r^i) A^{\beta j}(\mathbf{r}) r^j}{|\mathbf{r}|^3 |\mathbf{r}' - \mathbf{r}|^3} \Delta\mathbf{r}. \qquad (58)
\end{aligned}$$

We note that

$$\sum_{c=1}^{8} f^{\lambda bc} f^{c\beta\lambda} = -F(\lambda, b)\delta^{b\beta}, \qquad (59)$$

where $F(\lambda, b)$ is a non-negative quantity defined by

$$F(\lambda, b) = \sum_{c=1}^{8} (f^{\lambda bc})^2, \qquad (60)$$

which can be easily evaluated. For example, $F(1, b)$ is $\{0, 1, 1, 1/4, 1/4, 1/4, 1/4, 0\}$ for $b = 1, 2, \ldots, 8$. In terms of

$F(\lambda, b)$, the induced charge density is

$$\rho_{\rm ind}^{\lambda(2)}(\mathbf{r}', \mathbf{r})\Delta\mathbf{r} = -g^2 \sum_{b=1}^{8} F(\lambda, b)\Delta\mathbf{r} \times \sum_{i,j=1}^{3} \frac{A^{bi}(\mathbf{r}')A^{bj}(\mathbf{r})(r'^i - r^i)r^j}{|\mathbf{r}|^3|\mathbf{r}' - \mathbf{r}|^3}. \quad (61)$$

Note that $F(\lambda, \lambda) = 0$. The contribution of the external gauge field to the sum over b comes only from those color components of A^{bi} that are transverse to the color axis λ of the external point source.

The product $A^{bi}(\mathbf{r}')A^{bj}(\mathbf{r})$ in Eq. (61) involves spatial gauge fields at different spatial locations. Previously, Svetitsky, Yaffe, DeTar, and DeGrand found that large spacelike Wilson loops in the quark-gluon plasma have an area law behavior. Such a behavior indicates that the spatial gauge fields $A^{bj}(\mathbf{r})$ at different spatial locations are correlated [2,3,31,33,34]. As shown in the Appendix, if the gauge fields A^{bi} at different field points $\mathbf{r}_>$ and $\mathbf{r}_<$ with $|A^{bi}(\mathbf{r}_>)| > |A^{bi}(\mathbf{r}_<)|$ are correlated as

$$A^{bi}(\mathbf{r}_<) = A^{bi}(\mathbf{r}_>)e^{-|\mathbf{r}_> - \mathbf{r}_<|/\xi}, \quad (62)$$

then the integral of $A^{bi}(\mathbf{r})$ along a spacelike loop $\oint A^{bi}dx^i$ obeys an area law, when the linear dimensions of the loop are small compared with the correlation length. Consequently, within the vicinity of the correlation length ξ, we can express the thermal average of the $A^{bi}(\mathbf{r}')A^{bj}(\mathbf{r})$ in terms of the relative coordinate and the correlation length ξ:

$$\langle A^{bi}(\mathbf{r}')A^{bj}(\mathbf{r})\rangle \sim A^{bi}(\mathbf{r})A^{bj}(\mathbf{r})e^{-|\mathbf{r}' - \mathbf{r}|/\xi}, \quad (63)$$

where we have considered the case when $|A^{bi}(\mathbf{r}')| < |A^{bi}(\mathbf{r})|$. [The case of $|A^{bi}(\mathbf{r}')| > |A^{bi}(\mathbf{r})|$ can be treated in an analogous way.] The quenched QCD calculations in SU(3) is in the universal class of three-dimensional Z(3) symmetry. It has a first-order phase transition and it possesses a large but finite correlation length at T_c [2,3,31,33,34,82–86].

To study the sign of the induced color charges, we choose a spatial coordinate system with the z axis along $\mathbf{r}$ as shown in Fig. 11(a). In this coordinate system, we label the angular coordinates of $\mathbf{r}' - \mathbf{r}$ and $\mathbf{A}^b(\mathbf{r})$ by (θ', ϕ') and (θ_b, ϕ_b), respectively. We shall study the induced charge at $\mathbf{r}'$ within the vicinity of the correlation length ξ of $\mathbf{r}$. Then, after taking the thermal average, the induced color charge density is then

$$\rho_{\rm ind}^{\lambda(2)}(\mathbf{r}', \mathbf{r})\Delta\mathbf{r} = -g^2 \sum_{b=1}^{8} F(\lambda, b)\Delta\mathbf{r} \frac{|\mathbf{A}^b(\mathbf{r})|^2 e^{-|\mathbf{r}' - \mathbf{r}|/\xi}}{r^2|\mathbf{r}' - \mathbf{r}|^2} \times \cos\theta_b[\cos\theta_b \cos\theta' + \sin\theta_b \sin\theta' \cos(\phi_b - \phi')]. \quad (64)$$

If we average over the azimuthal angle ϕ', the second term in the square brackets drops out and we have

$$\rho_{\rm ind}^{\lambda(2)}(\mathbf{r}', \mathbf{r})\Delta\mathbf{r} = -g^2 \sum_{b=1}^{8} F(\lambda, b)\Delta\mathbf{r} \times \frac{|\mathbf{A}^b(\mathbf{r})|^2 \cos^2\theta_b e^{-|\mathbf{r}' - \mathbf{r}|/\xi} \cos\theta'}{r^2(r^2 + |\mathbf{r}' - \mathbf{r}|^2 + 2r|\mathbf{r}' - \mathbf{r}|\cos\theta')}. \quad (65)$$

One readily observes that the induced color charge density $\rho_{\rm ind}^{\lambda(2)}(\mathbf{r}', \mathbf{r})$ at $\mathbf{r}'$ is negative in the forward hemisphere in the direction forward of $\mathbf{r}$ (with $\pi/2 \geqslant \theta' \geqslant 0$). It changes to positive in the backward hemisphere, in the direction backward of $\mathbf{r}$ ($\pi \geqslant \theta' \geqslant \pi/2$). In the region of $\mathbf{r}'$ within the vicinity of the correlation length from $\mathbf{r}$, the induced charge surrounding $\mathbf{r}$ is a color-dipole-type density distribution with the color charge of the same sign at distances closer to the color source and of the opposite sign at distances farther to the color source [Fig. 11(b)]. This is the antiscreening behavior resulting from the presence of the external gauge field $A^{bi}(\mathbf{r})$ at $\mathbf{r}$. The magnitude of the induced color charges will increase with an increases in the correlation length ξ and the magnitude of the gluon field. The antiscreening effects will enhance the attractive interaction between the heavy quark and antiquark and will reduce the screening mass from the Debye screening predictions.

The antiscreening effect arises from the nonlinear properties of the non-Abelian gauge field whereas the effects of Debye screening arises from the interaction between the quark and antiquark with gluons. Both effects are present and the antiscreening effects resulting from deconfined gluons will act to counterbalance the effects of Debye screening. At the onset of the phase transition, the correlation length is large [2,3,31,33,34,82–88] and deconfined gluons are present; there can also be "remnants of the confinement part of QCD" at temperatures slightly above T_c, as pointed out by Kaczmarek *et al.* [79]. At a much higher temperature, a greater thermal fluctuation leads to a smaller correlation length, reducing the effects of antiscreening, and Debye screening dominates.

XI. DISSOCIATION OF J/ψ IN COLLISION WITH GLUONS

It is not necessary to reach the spontaneous dissociation temperature with zero binding energy for a quarkonium to dissociate. In a quark-gluon plasma, gluons and quarks can collide with a color-singlet heavy quarkonium to lead to the dissociation of the heavy quarkonium. Dissociation by the absorption of a single gluon is allowed as the color-octet final state of a free quark and a free antiquark can propagate in the color medium, in contrast to the situation below T_c in which the quark and the antiquark are confined. We shall consider dissociation of heavy quarkonium by gluons in the present work. The collision of a heavy quarkonium with light quarks can also lead to the dissociation of the heavy quarkonium, but through higher order processes. They can be considered in a future refined treatment of the dissociation process.

Previous treatment of the dissociation of heavy quarkonium by the absorption of a gluon was carried out by Peskin and Bhanot [89,90]. They use the operator product expansion and the large-N_c limit. They sum over a large set of diagrams and show that, to obtain gauge-invariant results, they need to sum over diagrams in which the external gluon is coupled to the gluon that is exchanged between the heavy quark and the heavy antiquark. They use the hydrogen wave function and hydrogen states to evaluate the transition matrix elements. Their expression for the dissociation cross section of $\sigma(g +$

$(Q\bar{Q})_{1S} \to Q + \bar{Q}$) is

$$\sigma(g + (Q\bar{Q})_{1S} \to Q + \bar{Q}) = \frac{2}{3}\pi \left(\frac{32}{3}\right)^2 \left(\frac{4}{3\alpha_s^2}\right) \frac{1}{m_Q^2} \frac{(E/B)^{3/2}}{(E/B+1)^5}. \quad (66)$$

where E is the nonrelativistic kinetic energy of the dissociated Q and $\bar{Q}$ in the center-of-mass system. In this short-distance approach of Peskin and Bhanot, the quark and the antiquark form a color-dipole pair and the gluons couple to the Wilson loop (the quarkonium) via simple dipole interactions. The dissociation cross section of Eq. (66) is, in fact, the dissociation of the quarkonium through the absorption of $E1$ gluon radiation.

Peskin and Bhanot's analytical result for the dissociation cross section has been applied to many calculations [23,24,91]. In heavy quarkonia of interest, the radial dependence of the quark-antiquark potential often differs from the Coulomb potential. The calculation of the dissociation cross section requires a new formulation, which can be best described by the potential model introduced previously [28,51], following the results of Blatt and Weisskopf [71] obtained for the photodisintegration of a deuteron. The dissociation process is schematically illustrated in Fig. 12. An initial bound $(Q\bar{Q})_{1S}$ state with a binding energy B in the color-singlet potential $V_1(r)$ absorbs a gluon of energy $\hbar\omega_g$ and is excited to the color-octet final state $(Q + \bar{Q})_{1P}$ with a kinetic energy E above the rest mass of $m_Q + m_{\bar{Q}}$. The interaction $V_8(r)$ between Q and $\bar{Q}$ in the color-octet state will be different from the interaction $V_1(r)$ in the color-singlet state, as shown in Fig. 12. At low energies, the dominant dissociation cross section is the $E1$ color-electric-dipole transition for which the final state of $Q + \bar{Q}$ will be in the 1P state in the continuum. The dissociation cross section $\sigma(g + J/\psi \to c + \bar{c})$ for such a color $E1$ transition can be obtained from the analogous result in QED [28,71], and the result is [28]

$$\sigma_{\rm dis}^{E1}(E_{\rm gluon}) = 4 \times \frac{\pi}{3}\alpha_{\rm gQ}(k^2 + \gamma^2)k^{-1}I^2, \quad (67)$$

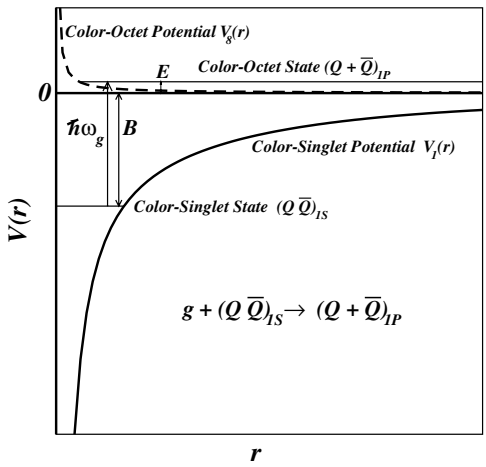

FIG. 12. The quarkonium dissociation process in the potential model.

where

$$E_{\rm gluon} = B + E, \quad \gamma^2 = 2\mu B, \quad k^2 = 2\mu E, \quad (68)$$

$$I = \int_0^\infty u_{1P}(r)\, r\, u_{1S}(r) dr, \quad (69)$$

$$\alpha_{\rm gQ} = \alpha_s \left| \langle 8c | \frac{\lambda^c}{2} | 1 \rangle \right|^2 = \alpha_s \times \frac{1}{6}, \quad (70)$$

and α_s is the gluon-(heavy quark) coupling leading to the dissociation of the heavy quarkonium. Here, we use the same notation and normalization as in Blatt and Weisskopf. The bound-state wave function u_{1S} has been normalized according to Eq. (49) as in Eq. (XII.4.18) of Blatt and Weisskopf [71], and the continuum wave function u_{1P} is normalized according to

$$u_{1P}(r)|_{r\to\infty} \to kr j_1(kr) = \frac{\sin(kr)}{kr} - \cos(kr), \quad (71)$$

as in Eq. (XII.4.32) of Blatt and Weisskopf [71]. The result from the potential model agrees with the analytical results of Bhanot and Peskin for the case they considered (hydrogen wave function, large-N_c limit,...) [28]. Such an agreement was further confirmed by numerical calculations according to Eq. (67) using the hydrogen wave function for u_{1S} and the plane wave continuum wave function for u_{1P}, as assumed by Peskin and Bhanot [89,90]. The potential model has the practical advantage that it can be used for a Q-$\bar{Q}$ system with a general potential.

XII. J/ψ COLLISIONAL DISSOCIATION RATE AND DISSOCIATION WIDTH

We have represented the color-singlet potential between a heavy quark and antiquark by a screened Coulomb potential and have obtained the J/ψ wave function. To study the gluon dissociation of J/ψ, we need the color-octet potential $V_8(\mathbf{r}, T) = U^{(8)}_{Q\bar{Q}}(\mathbf{r}, T)$ experienced by the Q and $\bar{Q}$ in the final state. We shall assume the generalization that the color dependence of the potential [Eq. (46)] is simply obtained by modifying the color factor from $-4/3$ for the color-singlet state to $1/6$ for the color-octet state:

$$U^{(i)}_{Q\bar{Q}}(\mathbf{r}, T) - U^{(i)}_{Q\bar{Q}}(\mathbf{r} \to \infty, T) = C_f \frac{f_F\alpha_F\, e^{-\mu_F r} + f_U\alpha_U\, e^{-\mu_U r}}{r}, \quad (72)$$

$$C_f = \begin{cases} -4/3 (i = 1, \text{color singlet}), \\ 1/6 (i = 2, \text{color octet}). \end{cases} \quad (73)$$

We also need the gluon-quark coupling constant α_s in Eq. (70) to evaluate the dissociation cross section. We shall consider the screened Coulomb potential (67) obtained in the lattice gauge theory as arising from the exchange of a virtual nonperturbative gluon and assume that the coupling of the gluon to the heavy quark leading to quarkonium bound states, $f_F\alpha_F + f_U\alpha_U$, is the same coupling leading to the dissociation of the quarkonium. The J/ψ dissociation cross section can then be calculated using Eq. (67). The results of the J/ψ dissociation cross section for different temperatures are shown

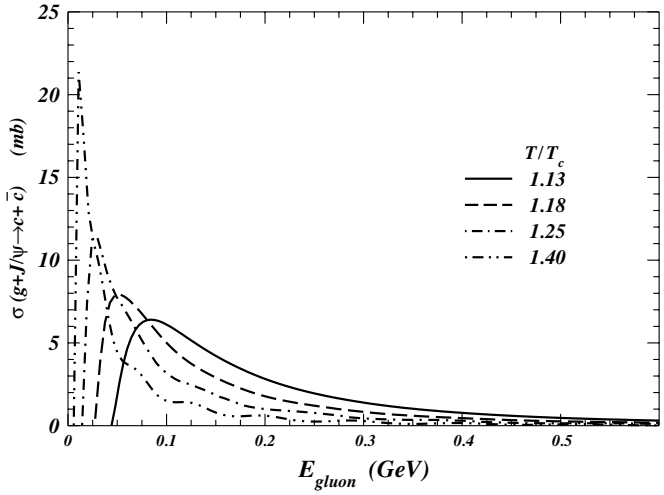

FIG. 13. J/ψ dissociation cross section as a function of gluon energy at various quark-gluon plasma temperatures.

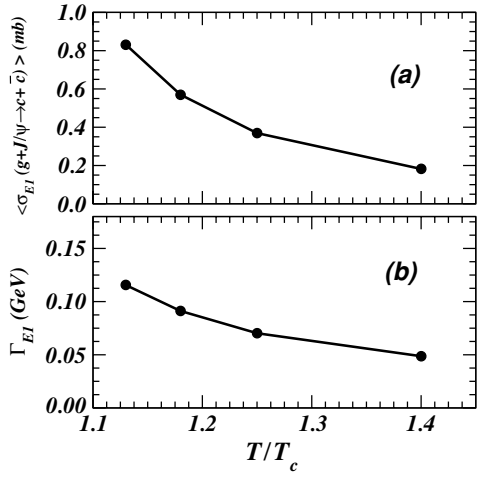

FIG. 14. (a) Thermally averaged dissociation cross section as a function of temperature. (b) J/ψ collisional dissociation width Γ_{E1} as a function of temperature.

in Fig. 13. The cross section increases up to a maximum value and decreases as the gluon energy increases. As the temperature decreases the maximum height of the dissociation cross section increases, but the width of the cross section decreases. We shall limit our attention to the dissociation of J/ψ by the absorption of $E1$ radiation in the present analysis. When the dissociation threshold decreases, higher multipole dissociation may become important. It will be of interest to study dissociation arising from gluon radiation of higher multipolarity in future work.

If we place a J/ψ in a quark-gluon plasma at a temperature T, the average $E1$ dissociation cross section is

$$\langle \sigma_{\rm dis}^{E1} \rangle = \frac{g_g}{2\pi^2} \int_0^\infty \sigma_{\rm dis}^{E1}(p) \frac{p^2 dp}{e^{p/T} - 1} \Big/ n_g, \tag{74}$$

where $g_g = 16$ is the gluon degeneracy and n_g is the gluon density, given by

$$n_g = \frac{g_g}{2\pi^2} \int_0^\infty \frac{p^2 dp}{e^{p/T} - 1}. \tag{75}$$

Using the energy dependence of the dissociation cross section as given in Fig. 13, we can calculate the average dissociation cross section $\langle \sigma_{\rm dis}^{E1} \rangle$. From $\langle \sigma_{\rm dis}^{E1} \rangle$, we obtain the rate of J/ψ dissociation (by $E1$ transition) given by

$$\frac{dn_{J/\psi}}{dt} = -n_g \langle \sigma_{\rm dis}^{E1} \rangle. \tag{76}$$

This dissociation rate leads to the collisional dissociation width Γ_{E1} resulting from the absorption of $E1$ gluon radiation,

$$\Gamma_{E1} = n_g \langle \sigma_{\rm dis}^{E1} \rangle. \tag{77}$$

We show in Fig. 14 the temperature dependence of $\langle \sigma_{\rm dis}^{E1} \rangle$ and Γ_{E1}. One observes that the average cross section is in the range of 0.2–0.8 mb. The collisional dissociation width resulting from $E1$ gluon absorption is of the order of 0.05–0.11 GeV, and the mean life of J/ψ in the quark-gluon plasma resulting from the absorption of gluons to the 1P state is therefore of order 2–4 fm/c.

XIII. J/ψ PRODUCTION BY THE COLLISION OF c AND $\bar{c}$ IN QGP

In high-energy nuclear collisions, elementary nucleon-nucleon collisions lead to the production of open heavy quark mesons. Although the probability for such a production is small for a single nucleon-nucleon collision, there are many nucleon-nucleon collisions in a central nucleus-nucleus collision. The large number of binary nucleon-nucleon collisions can produce many pairs of open charm mesons, and these open charm mesons can recombine to produce J/ψ. It is of interest to estimate the elementary reaction cross section for $c + \bar{c} \to J/\psi + g$ and obtain the rate of J/ψ production in a nucleus-nucleus collision.

The reaction $c + \bar{c} \to J/\psi + g$ is just the inverse of $g + J/\psi \to c + \bar{c}$. Their cross sections are therefore related by [92]

$$\sigma^{E1}(c + \bar{c} \to J/\psi + g) = \frac{|\boldsymbol{p}_1|^2}{|\boldsymbol{p}_3|^2} \sigma^{E1}(J/\psi + g \to c + \bar{c}), \tag{78}$$

where $\boldsymbol{p}_1$ is the momentum of one of the particles in the $J/\psi + g$ system, and $\boldsymbol{p}_3$ is the momentum of one of the particles in the $c + \bar{c}$ system, both measured in the center-of-mass frame. With Eq. (78) and the results of $\sigma^{E1}(J/\psi + g \to c + \bar{c})$ in Fig. 14, the production cross section $\sigma^{E1}(c + \bar{c} \to J/\psi + g)$ can be calculated. The cross section as a function of the kinetic energy of c and $\bar{c}$ in the center-of-mass system are shown in Fig. 15. One observes that the cross section peaks at low kinetic energies near the threshold, and the magnitude of the cross section decreases with temperature. The maximum cross section at $T/T_c \sim 1.13$ is of order 0.7 mb.

The rate of J/ψ production can be obtained when the momentum distribution $f(y, \boldsymbol{p}_t)$ of the produced c and $\bar{c}$ is known. For simplicity, we consider charm quarks and antiquarks to be contained in a spatial volume V with a uniform distribution. The probability of producing a J/ψ in the volume V per unit time by the collision of charm quark and antiquark is

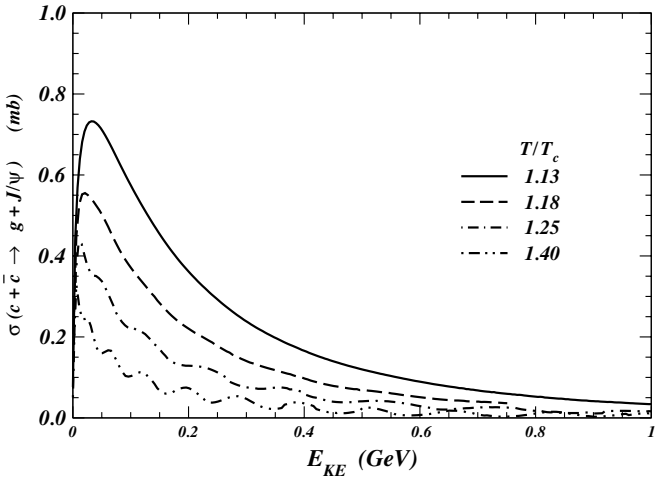

FIG. 15. Cross section for the production of J/ψ by the collision of c and $\bar{c}$.

$\sigma(c+\bar{c}\to J/\psi+g)v_{12}/V$, where v_{12} is the relative velocity between c and $\bar{c}$. The number of J/ψ produced per unit time from collision of c and $\bar{c}$ is therefore

$$\frac{dN_{J/\psi}}{dt}=\int dy_1 d\boldsymbol{p}_{1t} dy_2 d\boldsymbol{p}_{2t} f(y_1,\boldsymbol{p}_{1t}) f(y_2,\boldsymbol{p}_{2t}) \times \sigma(c+\bar{c}\to J/\psi+g)v_{12}/V. \quad (79)$$

When we neglect initial- and final-state interactions, the momentum distribution of charm is given by

$$f(y,\boldsymbol{p}_t)=N_{\rm bin}\frac{Ed N_{c\bar{c}}^{pp}}{d\boldsymbol{p}}. \quad (80)$$

Here $f(y,\boldsymbol{p}_t)$ is normalized to the total number of charm quarks N_c and antiquarks $N_{\bar{c}}$ produced in the nucleus-nucleus collision, $N_c=N_{\bar{c}}=\int(d\boldsymbol{p}/E)f(y,\boldsymbol{p}_t)=N_{\rm bin}N_{c\bar{c}}^{pp}$, $N_{\rm bin}$ is the number of binary nucleon-nucleon collisions, and $N_{c\bar{c}}^{pp}$ is the number of c-$\bar{c}$ pairs produced in a single nucleon-nucleon collision. From the charm production data in d-Au collisions and PYTHIA calculations, Tai *et al.* [93], Adams *et al.* [94], and the STAR Collaboration inferred that at $\sqrt{s}=200$ GeV the charm production cross section per nucleon-nucleon collision is $\sigma_{c\bar{c}}^{pp}|_{\rm STAR}=1.18\pm0.21({\rm stat})\pm 0.39({\rm sys})$ mb [93] and $\sigma_{c\bar{c}}^{pp}|_{\rm STAR}=1.4\pm0.2\pm0.4$ mb [94]. If one uses the transverse momentum distribution measured and parametrized by Tai *et al.* [93] and assumes a Gaussian rapidity distribution, the charm momentum distribution of Adams *et al.* [94] per nucleon-nucleon collision can be represented by

$$\frac{Ed N_{c\bar{c}}^{pp}}{d\boldsymbol{p}}({\rm PYTHIA(STAR)})=\frac{Ed\sigma_{c\bar{c}}^{pp}\big|_{\rm STAR}}{\sigma_{\rm in}d\boldsymbol{p}}=A\frac{e^{-y^2/2\sigma_y^2}}{(1+p_t/p_{t0})^n}, \quad (81)$$

where $\sigma_{\rm in}=42$ mb is the nucleon-nucleon inelastic cross section, $A=4.4\times10^{-3}$ GeV^{-2}, $\sigma_y=1.84$, $p_{t0}=3.5$ GeV, and $n=8.3$. The number of $c\bar{c}$ pairs produced per nucleon-nucleon collision is $N_{c\bar{c}}^{pp}|_{\rm STAR}=1.4$ mb/42 mb $=0.033\pm0.0107$.

The PHENIX Collaboration obtained $\sigma_{c\bar{c}}^{pp}|_{\rm PHENIX}=622\pm 57({\rm stat})\pm160({\rm sys})$ μb [95] for the open charm production cross section per nucleon-nucleon collision at $\sqrt{s}=200$ GeV, and $N_{c\bar{c}}^{pp}|_{\rm PHENIX}=0.0148\pm0.004$. With this total charm production cross section, the theoretical results from the PYTHIA calculations of the PHENIX Collaboration can be parametrized as [95,96]

$$\frac{Ed N_{c\bar{c}}^{pp}}{d\boldsymbol{p}}({\rm PYTHIA(PHENIX)})=A'\frac{e^{-y^2/2\sigma_y'^2}}{(1+p_t/p_{t0}')^{n'}}, \quad (82)$$

where $A'=6.48\times10^{-4}$ GeV^{-2}, $\sigma_y'=1.85$, $p_{t0}'=5.06$ GeV, and $n'=7.0$.

We shall focus attention on central Au-Au collisions within the most inelastic 10% of the reaction cross section. The average number of binary collisions for these central Au-Au collisions at RHIC is $N_{\rm bin}=833$. For these central nucleus-nucleus collisions at $\sqrt{s}=200$ GeV, the average numbers of c and $\bar{c}$ produced are $N_c=N_{\bar{c}}=27.8\pm8.9$, if we use the cross section of the STAR Collaboration [94], and $N_c=N_{\bar{c}}=12.34\pm3.4$, if we use the cross section of the PHENIX Collaboration [95]. The rate of J/ψ production can then be obtained from Eqs. (79)–(82) by carrying out the sixfold integration.

In Fig. 16 we show the quantity $VdN_{J/\psi}/dt$ as a function of temperature for the most inelastic (10%) central Au-Au collisions at $\sqrt{s}=200$ GeV. The estimate of the rate of J/ψ production, using the momentum distribution of Eq. (81) from the PYTHIA calculations of the STAR Collaboration [94], is greater than the corresponding estimate, using the momentum distribution of Eq. (82) from the PYTHIA calculations of the PHENIX Collaboration [94,96], by a factor of about 10. This factor is larger than the factor of 2.25 of the nucleon-nucleon $c\bar{c}$ production cross section of the STAR Collaboration, relative to the corresponding cross section of the PHENIX Collaboration at $\sqrt{s}=200$ GeV. The large difference of these two factors arises because the charm momentum distribution from the PYTHIA calculations of the STAR Collaboration has a greater

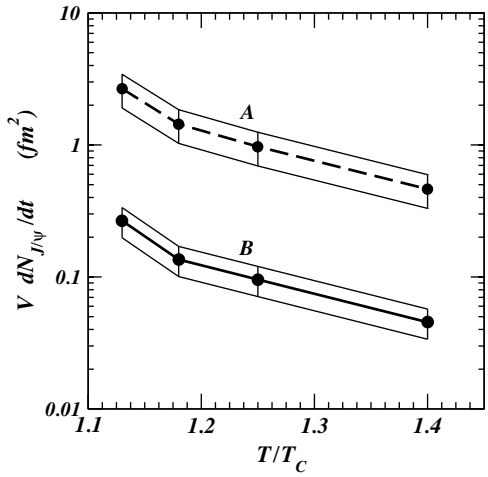

FIG. 16. The rate of J/ψ production as a function of temperature, for the most inelastic (10%) central Au-Au collision at $\sqrt{s}=200$ GeV. Curve A is based on the charm momentum distribution of Eq. (81) using the PYTHIA calculations of the STAR Collaboration [94]; curve B is based on the charm momentum distribution of Eq. (82) using the PYTHIA calculations of the PHENIX Collaboration [94,96].

magnitude at low p_T, and c and $\bar{c}$ recombine more readily at low relative energies, as indicated in Fig. 16.

We can illustrate the magnitude of the rate of J/ψ production by considering a Au-Au central collision with a transverse area of $\pi(7\ \mathrm{fm})^2$ and a longitudinal initial time (and longitudinal length) of 1 fm. The initial volume containing the charm quarks and antiquarks is about 150 fm^3. If the initial temperature is $1.4T_c$, the initial rate of J/ψ production will be about 3×10^{-4} to 3×10^{-3} fm/c. As the volume expands, the temperature decreases. The results of Fig. 16 can be used to provide an estimate of the rate of J/ψ production.

XIV. DISCUSSION AND CONCLUSIONS

We use the color-singlet free energy F_1 and internal energy U_1 obtained by Kaczmarek *et al.* [22] in quenched QCD to study the energy levels of charmonium and bottomium above the phase-transition temperature. From a variational principle in a schematic model, we find that the Q-$\bar{Q}$ potential involves only the Q-$\bar{Q}$ internal energy $U^{(1)}_{Q\bar{Q}}$, which can be obtained from the total U_1 by subtracting the gluon internal energy contributions. We carry out this subtraction using the local energy-density approximation in which the gluon energy density can be related to the local gluon pressure by the quark-gluon plasma equation of state. We find that the Q-$\bar{Q}$ potential is $U^{(1)}_{Q\bar{Q}} = 3F_1/(3+a) + aU_1/(3+a)$, where $a = 3p/\epsilon$ is given by the quark-gluon plasma equation of state. Such a $U^{(1)}_{Q\bar{Q}}$ potential leads to weakly bound J/ψ and η_c at temperatures above the phase-transition temperature and they become unbound at $1.62T_c$. The χ_c, η_c', and ψ' states are found to be unbound in the quark-gluon plasma. In this potential model, Υ, η_b, Υ', η_b', and χ_b are bound at temperatures above T_c; Υ and η_b dissociate spontaneously at $4.10T_c$, χ_b at $1.18T_c$, and Υ' and η_b' at $1.38T_c$.

The results from the $U^{(1)}_{Q\bar{Q}}$ potential need to be tested against results from spectral function analysis. For completeness, we have also calculated heavy quarkonium binding energies using the free energy F_1 [25–28] and the total internal energy U_1 as the potential [8,29,30].

The comparison shows that different models give very different heavy quarkonium binding energies. The potential that agrees best with results obtained from spectral function analysis is the $U^{(1)}_{Q\bar{Q}}$ potential deduced in the present analysis. The agreement with spectral function analysis and the theoretical foundations presented here provide support for the use of $U^{(1)}_{Q\bar{Q}}$ as the proper Q-$\bar{Q}$ potential in heavy quarkonium studies. Conversely, the agreement also lends support to the quantitative features concerning the stability of heavy quarkonia in the spectral function analyses of Asakawa *et al.* [9,10] and Petreczky *et al.* [11–13].

The spectral function analysis for the bottomium states has not yet been carried out. Because the predications for the dissociation temperatures for bottomium states are quite different from different potential models, it will be of great interest to calculate the bottomium dissociation temperatures in lattice gauge spectral function analysis so as to test the potential models further.

In a nucleus-nucleus collision, charm quarks and antiquarks are produced in hard-scattering processes in nucleon-nucleon collisions. During the time of a central nuclear reaction, these heavy quarks and antiquarks will be present in the quark-gluon plasma and can interact to form J/ψ. We have calculated the cross section for J/ψ production by the collision of a charm quark and an antiquark. The cross section is energy dependent, and the maximum cross section increases as the temperature decreases. The production cross section can be used to study the rate of J/ψ production in nucleus-nucleus collisions.

We have carried out the investigation using the quenched QCD. It will be of interest to carry out similar investigations using unquenched QCD. Results of the full QCD in two flavors [70] and in three flavors [97] have been obtained recently, and an investigation on J/ψ dissociation temperatures in QCD with two flavors has been initiated [15]. A thorough study of how the dynamical quarks will affect the stability, the dissociation, and the inverse production of heavy quarkonium will be of great interest.

It is necessary to emphasize that the present Q-$\bar{Q}$ potential $U^{(1)}_{Q\bar{Q}}$ of Eq. (43) extracted from F_1 and U_1 has been obtained in the local energy-density approximation. It would be of great interest in future lattice gauge calculations to evaluate the $U^{(1)}_{Q\bar{Q}}(\mathbf{r})$ directly to check the validity of the local energy-density approximation.

The color-singlet correlator of the Polyakov lines in Eq. (1) is not gauge invariant. It has been suggested that one can dress the Polyakov lines to make a gauge-invariant definition of the color-singlet potential. The dressing of the source may be viewed as a gauge transformation and is equivalent to the choice of a certain gauge [98] with the requirement that the gauge-fixed Polyakov loop correlation function in the singlet channel falls off with gauge-invariant eigenvalues of the Hamiltonian. This requirement may be satisfied for the Coulomb gauge and other time-local gauges. Recent calculations by Belavin *et al.* [99] show however that the color-singlet potential depends on the choice of the gauges even among these time-local gauges. It has been found that at finite temperatures all channels receive contributions only from the color-singlet channel. The extraction of the color-singlet potential from the "color-singlet" Polyakov correlator of Eq. (1) may include additional r and/or T dependence, which is not shared by the physical states [100]. Clearly, much work remains to be carried out to clarify the proper color-singlet potential in lattice gauge calculations.

ACKNOWLEDGMENTS

The authors would like to thank Drs. H. Crater, P. Petreczky, M. Gyulassy, Su Houng Lee, Keh-Fei Liu, T. Barnes, S. Ohta, V. Cianciolo, D. Silvermyr, Huan Huang, and Zhangbu Xu for helpful discussions and communications. This research was supported in part by the Division of Nuclear Physics, U.S. Department of Energy, under Contract No. DE-AC05-00OR22725, managed by UT-Battelle, LLC, and by the National Science Foundation under Contract No. NSF-Phy-0244786 at the University of Tennessee.

APPENDIX: SPACELIKE AREA LAW AND THE CORRELATION OF GAUGE FIELDS

We focus our attention on the x–y plane so that the z coordinate can be omitted and consider a loop integral $\oint_L A_i dx^i$ along the loop L defined by $(0,0) \to (L_x,0) \to (L_x,L_y) \to (0,L_y) \to (0,0)$. The integral around this loop of area $L_x L_y$ is given approximately by

$$\oint_L A_i dx^i = A_x\left(\frac{L_x}{2},0\right)L_x + A_y\left(L_x,\frac{L_y}{2}\right) \times L_y - A_x\left(\frac{L_x}{2},L_y\right)L_x - A_y\left(0,\frac{L_y}{2}\right)L_y. \tag{A1}$$

We can write the right-hand side in the form

$$\oint_L A_i dx^i = cL_xL_y, \tag{A2}$$

where

$$c = \frac{A_x(L_x/2,0) - A_x(L_x/2,L_y)}{L_y} - \frac{A_y(L_x,L_y/2) - A_y(0,L_y/2)}{L_x}. \tag{A3}$$

If the gauge fields $\mathbf{A}$ at different field points are correlated by a correlation length ξ such that for two points $\mathbf{r}_>$ and $\mathbf{r}_<$ where $|A_i(\mathbf{r}_>)| > |A_i(\mathbf{r}_<)|$ and

$$A_i(\mathbf{r}_<) = A_i(\mathbf{r}_>)\, e^{-|\mathbf{r}_> - \mathbf{r}_<|/\xi}, \tag{A4}$$

then we have

$$\frac{A_x(L_x/2,0) - A_x(L_x/2,L_y)}{L_y} = \begin{cases} (1-e^{-L_y/\xi})A_x\left(\frac{L_x}{2},0\right)\big/L_y \text{ if } A_x\left(\frac{L_x}{2},0\right) > A_x\left(\frac{L_x}{2},L_y\right), \\ (e^{-L_y/\xi}-1)A_x\left(\frac{L_x}{2},L_y\right)\big/L_y \text{ if } A_x\left(\frac{L_x}{2},0\right) < A_x\left(\frac{L_x}{2},L_y\right). \end{cases} \tag{A5}$$

The second term in Eq. (A3) can be similarly evaluated. In the case of a correlation length ξ that is large compared with the loop lengths L_x and L_y, the quantity c in Eq. (A2) can be evaluated and we obtain the area law

$$\oint_L A_i dx^i = \frac{1}{\xi}(A_x^> - A_y^>)L_xL_y, \tag{A6}$$

where

$$A_x^> = \begin{cases} A_x(L_x/2,0) & \text{if} \quad A_x(L_x/2,0) > A_x(L_x/2,L_y), \\ -A_x(L_x/2,L_y) & \text{if} \quad A_x(L_x/2,0) < A_x(L_x/2,L_y) \end{cases} \tag{A7}$$

and

$$A_y^> = \begin{cases} A_y(0,L_y/2) & \text{if} \quad A_y(0,L_y/2) > A_y(L_x,L_y/2), \\ -A_y(0,L_y) & \text{if} \quad A_y(0,L_y/2) < A_y(L_x,L_y/2). \end{cases} \tag{A8}$$

Equation (A6) shows that if spacelike gauge fields at different points are correlated by Eq. (A4) with a large correlation length, the integral of the gauge fields along a spacelike Polyakov loop will satisfy an area law.

[1] T. Matsui and H. Satz, Phys. Lett. **B178**, 416 (1986).
[2] C. DeTar, Phys. Rev. D **32**, 276 (1985).
[3] C. DeTar, Phys. Rev. D **37**, 2328 (1988).
[4] T. H. Hansson, S. H. Lee, and I. Zahed, Phys. Rev. D **37**, 2672 (1988).
[5] Yu. A. Simonov, Phys. At. Nucl. **58**, 309 (1995) [Yad. Fiz. **58**, 357 (1995)].
[6] Yu. A. Simonov, Lecture at the International School of Physics "Enrico Fermi," Varenna, 27 June–7 July 1995, hep-ph/9509404.
[7] Yu. A. Simonov, Phys. Lett. **B619**, 293 (2005).
[8] F. Karsch and E. Laermann, chapter to appear in *Quark-Gluon Plasma III*, edited by R. Hwa, hep-lat/0305025.
[9] M. Asakawa, T. Hatsuda, and Y. Nakahara, Nucl. Phys. **A715**, 863 (2003).
[10] M. Asakawa and T. Hatsuda, Phys. Rev. Lett. **92**, 012001 (2004).
[11] P. Petreczky, S. Datta, F. Karsch, and I. Wetzorke, hep-lat/0309012.
[12] S. Datta, F. Karsch, P. Petreczky, and I. Wetzorke, Phys. Rev. D **69**, 094507 (2004).
[13] P. Petreczky, J. Phys. G **30**, S431 (2004).
[14] E. V. Shuryak and I. Zahed, Phys. Rev. C **70**, 021901(R) (2004).
[15] E. V. Shuryak and I. Zahed, Phys. Rev. D **70**, 054507 (2004).
[16] E. V. Shuryak, Nucl. Phys. **A750**, 64 (2005).
[17] E. V. Shuryak and I. Zahed, hep-ph/0406100.
[18] T. Hatsuda and T. Kunihiro, Phys. Rev. Lett. **55**, 158 (1985); T. Hatsuda and T. Kunihiro, Prog. Theor. Phys. **74**, 765 (1985).
[19] L. Grandchamp, R. Rapp, and G. E. Brown, J. Phys. G **30**, S1355 (2004).
[20] P. Petreczky, invited plenary talk presented at Hard Probes 2004, International Conference on Hard and Electromagnetic Probes of High Energy Nuclear Collisions, Nov. 4–10, 2004, Ericeira, Portugal. hep-lat/0502008.
[21] F. Karsch, Contribution to the Proceedings of Hard Probes 2004, International Conference on Hard and Electromagnetic Probes of High Energy Nuclear Collisions, Nov. 4–10, 2004, Ericeira, Portugal. hep-lat/0502014.
[22] O. Kaczmarek, F. Karsch, P. Petreczky, and F. Zantow, hep-lat/0309121.
[23] R. L. Thews, M. Schroedter, and J. Rafelski, Phys. Rev. C **63**, 054905 (2001).
[24] R. L. Thews and J. Rafelski, Nucl. Phys. **A698**, 575 (2002).
[25] S. Digal, P. Petreczky, and H. Satz, Phys. Lett. **B514**, 57 (2001).
[26] S. Digal, P. Petreczky, and H. Satz, Phys. Rev. D **64**, 094015 (2001).
[27] C. Y. Wong, Phys. Rev. C **65**, 034902 (2002).
[28] C. Y. Wong, J. Phys. G **28**, 2349 (2002).
[29] O. Kaczmarek, F. Karsch, and P. Petreczky, and F. Zantow, Phys. Lett. **B543**, 41 (2002).
[30] F. Zantow, O. Kaczmarek, F. Karsch, and P. Petreczky, hep-lat/0301015.
[31] L. G. Yaffe and B. Svetitsky, Phys. Rev. D **26**, 963(R) (1982).
[32] R. P. Feynman and A. R. Hibbs, *Quantum Mechanics and Path Integrals* (McGraw-Hill, New York, 1965), p. 276.

[33] B. Svetitsky and L. Yaffe, Nucl. Phys. **B210**, 423 (1982).
[34] T. A. DeGrand and C. E. DeTar, Phys. Rev. D **34**, 2469 (1986).
[35] K. H. Ackermann *et al*. (STAR Collaboration), Phys. Rev. Lett. **86**, 402 (2001); C. Adler *et al*. (STAR Collaboration), Phys. Rev. Lett. **87**, 182301 (2001); R. Snellings, for the STAR Collaboration, Nucl. Phys. **A698**, 193c (2002).
[36] R. A. Lacey, for the PHENIX Collaboration, Nucl. Phys. **A698**, 559c (2002); K. Adcox *et al*. (PHENIX Collaboration), nucl-ex/0204005.
[37] I. C. Park, for the PHOBOS Collaboration, Nucl. Phys. **A698**, 564c (2002).
[38] P. F. Kolb, J. Sollfrank, and U. Heinz, Phys. Lett. **B459**, 667 (1999); Phys. Rev. C **62**, 054909 (2000); P. F. Kolb, P. Huovinen, U. Heinz, and H. Heiselberg, Phys. Lett. **B500**, 232 (2001); P. F. Kolb, U. Heinz, P. Huovinen, K. J. Eskola, and K. Tuominen, Nucl. Phys. **A696**, 197 (2001); P. Huovinen, P. F. Kolb, U. Heinz, P. V. Ruuskanen, and S. A. Voloshin, Phys. Lett. **B503**, 58 (2001); P. Kolb and U. Heinz, Invited review for "Quark Gluon Plasma 3," edited by R. C. Hwa and X.-N. Wang (World Scientific, Singapore, 2003).
[39] T. Hirano, Phys. Rev. C **65**, 011901(R) (2002); T. Hirano and K. Tsuda, Phys. Rev. C **66**, 054905 (2002); T. Hirano, Invited talk given at XXXIV International Symposium on Multiparticle Dynamics, Sonoma, California, USA, July 26–August 1, 2004.
[40] D. Teaney, J. Lauret, and E. V. Shuryak, Phys. Rev. Lett. **86**, 4783 (2001); D. Teaney, J. Lauret, and E. V. Shuryak, nucl-th/0110037; D. Teaney, Phys. Rev. C **68**, 034913 (2003).
[41] L. D. Landau, Izv. Akad. Nauk SSSR **17**, 52 (1953); L. D. Landau and S. Z. Belenkij, Usp. Fiz. Nauk. **56**, 309 (1955).
[42] P. Carruthers, and M. Duong-Van, Phys. Rev. D **8**, 859 (1973).
[43] M. Murray, the BRAHMS Collaboration, J. Phys. G **30**, S667 (2004).
[44] S. M. H. Wong, hep-ph/0404222.
[45] D. Molnar and M. Gyulassy, talk given at International Symposium on Multiparticle Dynamics, October 9–15, 2000, Tihany, Hungary. D. Molnar and M. Gyulassy, Nucl. Phys. **A698**, 379 (2002); D. Molnar and M. Gyulassy, Nucl. Phys. **A697**, 495 (2002).
[46] E. Shuryak, Prog. Part. Nucl. Phys. **53**, 273 (2004).
[47] M. Gyulassy and L. McLerran, Nucl. Phys. **A750**, 30 (2005).
[48] *New Discoveries at RHIC: The Current Case for the Strongly Interactive QGP*, RIKEN Scientific Articles, Volume 9, BNL, May 14–15, 2004, published in Nucl. Phys. **A750**, issue 1, 1–170, edited by D. Rischke and G. Levin, 2005.
[49] Z.- W. Lin, C. M. Ko, and S. Pal, Phys. Rev. Lett. **89**, 152301 (2002).
[50] G. T. Bodwin, E. Braaten, and G. P. Lepage, Phys. Rev. D **51**, 1125 (1995).
[51] C. Y. Wong, Phys. Rev. D **60**, 114025 (1999).
[52] T. Appelquist, M. Dine, and I. Muzinich, Phys. Lett. **B69**, 231 (1977).
[53] S. Love, Ann. Phys. (NY) **113**, 153 (1978).
[54] R. Barbieri, M. Ciafaloni, and P. Menotti, Nuovo Cimento A **55**, 701 (1968).
[55] V. B. Berestetskii, E. M. Lifshitz, and L. Pitaevskii, *Quantum Electrodynamics* (Pergamon, New York, 1982).
[56] Y. Oh, S. Kim, and S. H. Lee, Phys. Rev. C **65**, 067901 (2002).
[57] J. des Cloizeaux, in *Many-Body Physics*, edited by C. de Witt and R. Balien (Gordon and Breach, New York, 1968).
[58] R. Balian, *Méchanque Statisique* (Hermann, Paris, 1980).
[59] P. Bonche and D. Vautherin, Nucl. Phys. **A372**, 496 (1981).
[60] P. Bonche, S. Levit, and D. Vautherin, Nucl. Phys. **A427**, 278 (1984).
[61] P. Bonche, S. Levit, and D. Vautherin, Nucl. Phys. **A436**, 265 (1985).
[62] D. Vantherin and D. Brink, Phys. Rev. C **5**, 626 (1972).
[63] C. Y. Wong and H. H. K. Tang, Phys. Rev. C **20**, 1419 (1979); C. Y. Wong, Phys. Rev. C **25**, 1460 (1982).
[64] The analogous case of using the photon chemical potential to study the total number of photons can be found in L. D. Landau and E. M. Lifshitz, *Statistical Physics, Part I* (Pergamon, New York, 1980), p. 184.
[65] C. Y. Wong, J. A. Maruhn, and T. A. Welton, Nucl. Phys. **A253**, 469 (1975); C. Y. Wong, J. Math. Phys. **17**, 1008 (1975); C. Y. Wong, J. A. Maruhn, and T. A. Welton, Phys. Rev. C **15**, 1558 (1977); C. Y. Wong and J. A. McDonald, Phys. Rev. C **16**, 1196 (1977); C. Y. Wong, and H. H. K. Tang, Phys. Rev. C **20**, 1419 (1979).
[66] C. W. Misner, J. A. Wheeler, and K. S. Thorne, *Gravitation*, (Freeman, San Francisco, 1970), p. 566.
[67] S. Weinberg, *Gravitation and Cosmology* (Wiley, New York, 1972), p. 128.
[68] G. Boyd, J. Engles, F. Karsch, E. Laermann, C. Legland, M. Lütgemeier, and B. Petersson, Nucl. Phys. **B469**, 419 (1996).
[69] K. Hagiwara *et al*. (Particle Data Group), Phys. Rev. D **66**, 010001 (2002).
[70] O. Kaczmarek, S. Ejiri, F. Karsch, E. Laermann, and F. Zantow, talk given at Finite Density QCD, Nara, Japan, 10–12 July, 2003, hep-lat/0312015.
[71] J. M. Blatt and V. F. Weisskopf, *Theoretical Nuclear Physics* (Wiley, New York, 1952), Eq. (VIII.2.63), p. 334.
[72] C. Y. Wong, E. S. Swanson, and T. Barnes, Phys. Rev. C **65**, 014903 (2001).
[73] V. V. Klimov, Yad. Fiz. **33**, 1734 (1981) [Sov. J. Nucl. Phys. **33**, 934 (1981)].
[74] H. A. Weldon, Phys. Rev. D **26**, 2789 (1982).
[75] J. I. Kapusta, *Finite Temperature Field Theory* (Cambridge University Press, Cambridge, England, 1989).
[76] E. Braaten and R. D. Pisarski, Phys. Rev. D **45**, 1827(R) (1992).
[77] A. Rebhan, Phys. Rev. D **48**, 3967(R) (1993).
[78] F. Karsch, lectures given at 40th Internationale Universitatswochen fuer Theoretische Physik: Dense Matter (IUKT 40), Schladming, Styria, Austria, 3–10 Mar 2001, hep-lat/0106019.
[79] O. Kaczmarek, F. Karsch, F. Zantow, and P. Petreczky, Phys. Rev. D **70**, 074505 (2004).
[80] K. Gottfried and V. F. Weisskopf, *Concepts of Particle Physics* (Oxford University Press, New York, 1986), Vol. II, p. 385.
[81] M. Peskin and D. V. Schroeder, *An Introduction to Quantum Field Theory* (Addison-Wesley, Reading, Massachusetts, 1996), p. 542.
[82] J. B. Kogut *et al*., Phys. Rev. Lett. **50**, 393 (1983).
[83] C. DeTar and J. Kogut, Phys. Rev. Lett. **59**, 399 (1987); Phys. Rev. D **36**, 2828 (1987); S. Gottlieb, W. Liu, D. Toussalnt, R. L. Renken, and R. L. Sugar, Phys. Rev. Lett. **59**, 1881 (1987).
[84] M. Fukugita, M. Otawa, and A. Ukawa, Phys. Rev. Lett. **63**, 1768 (1989).
[85] K. Holland, M. Pepe, and U.-J. Wiese, Nucl. Phys. **B694**, 35 (2004).
[86] F. Karsch, E. Laermann, and M. Lütgemeier, Phys. Lett. **B346**, 94 (1995).
[87] S. H. Lee, Phys. Rev. D **40**, 2484 (1989).

[88] J. M. Yeomans, *Statistical Mechanics of Phase Transitions* (Clarendon, Oxford, 1992).
[89] M. E. Peskin, Nucl. Phys. **B156**, 365 (1979).
[90] G. Bhanot and M. E. Peskin, Nucl. Phys. **B156**, 391 (1979).
[91] D. Kharzeev and H. Satz, Phys. Lett. **B334**, 155 (1994).
[92] Page 337 of Ref. [71].
[93] A. Tai, the STAR Collaboration, J. Phys. G **30**, S809 (2004).
[94] J. Adams, *et al*., the STAR Collaboration, Phys. Rev. Lett. **94**, 062301 (2005).
[95] S. S. Adler, the PHENIX Collaboration, nucl-ex/0409028.
[96] The author would like to thank Drs. D. Silvermyr and V. Cianciolo for providing the parametrization of the $c\bar{c}$ distribution, Eq. (82).
[97] P. Petreczky and K. Petrov, Phys. Rev. D **70**, 054503 (2004).
[98] O. Philipsen, Phys. Lett. **B535**, 138 (2002).
[99] V. A. Belavin, V. G. Bornyakov, and V. K. Mitrjushkin, Phys. Lett. **B579**, 109 (2004).
[100] O. Jahn and O. Philipsen, Phys. Rev. D **70**, 074504 (2004).